Insights into exotic hadrons from quark model

Qiang Zhao

Division of Theoretical Physics

Institute of High Energy Physics, CAS

zhaoq@ihep.ac.cn

Strong QCD 2024

Strong QCD from Hadron Structure Experiments - VI

2024.05.14-17., 南京

Outline

1. Hadrons beyond the conventional quark model
2. Questions from the quark model: where are the genuine color-singlet multiquark states?
3. Quark model states vs. hadronic molecules
4. Some crucial issues to be noted

1. Hadrons beyond the conventional quark model

Exotics of Type-I:

J^{PC} are not allowed by $Q\bar{Q}$ configurations, e.g. $0^{--}, 1^{-+}$ …

- Direct observation

Exotics of Type-II:

J^{PC} are the same as $Q\bar{Q}$ configurations

- Outnumbering of conventional QM states?
- Peculiar properties?

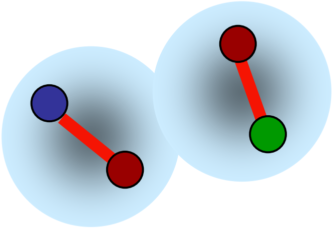

"Exotics" of Type-III:

Leading kinematic singularity can cause measurable effects, e.g. the triangle singularity.

- What's the impact?
- How to distinguish a genuine state from kinematic effects?

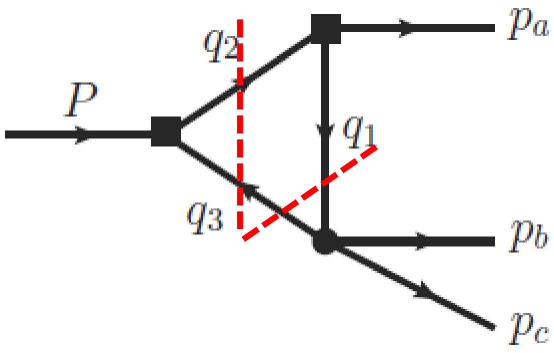

Production processes in experiment

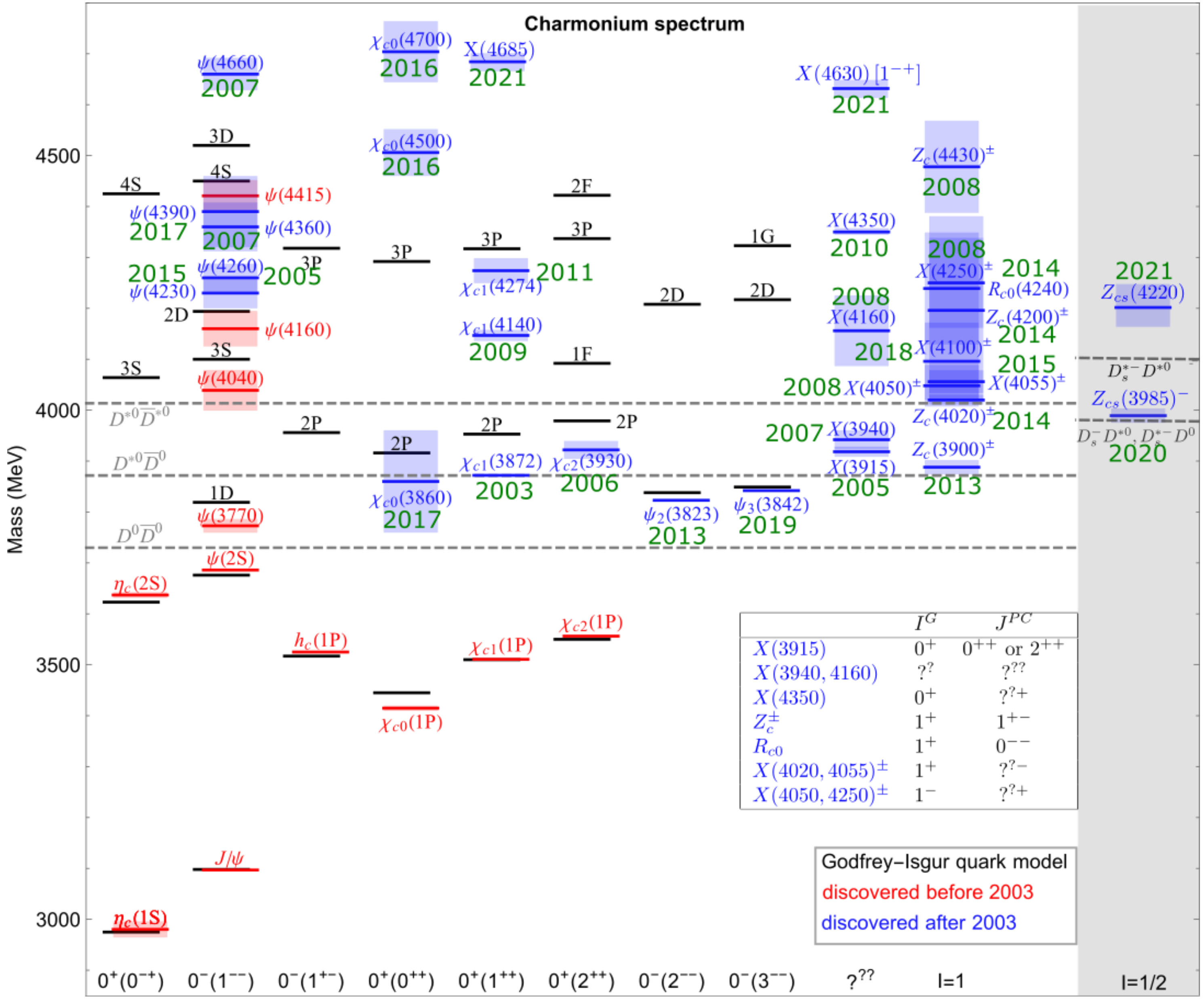

Chart plotted by Fengkun Guo

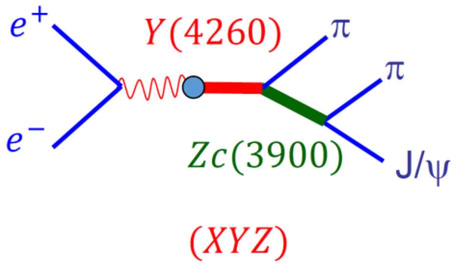

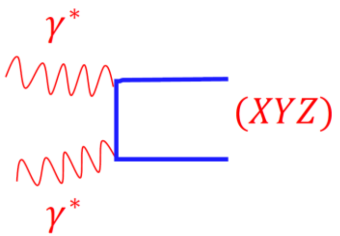

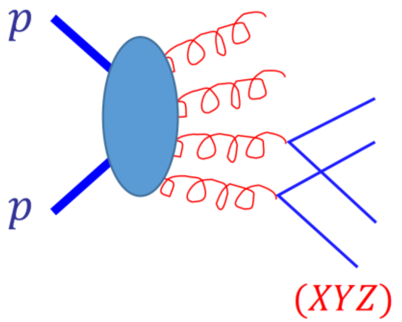

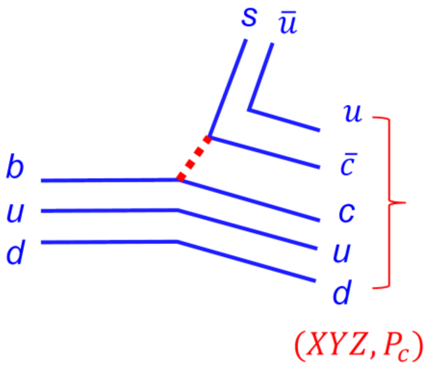

Genuine color-singlet multiquark states *vs.* hadron molecules

Tetraquark vs. hadronic molecule

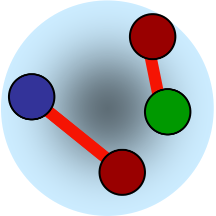

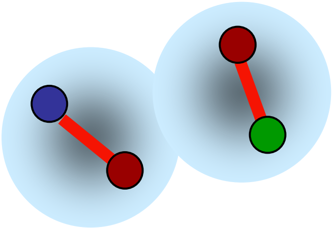

Pentaquark vs. hadronic molecule

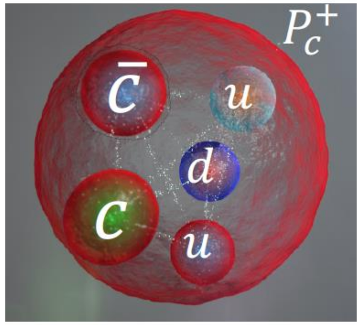

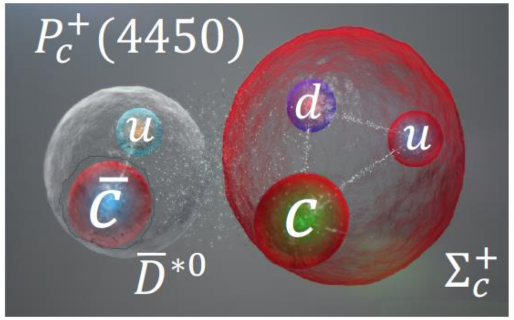

Status rating	
****	$X(3872), Z_c(3900)$
***	$Y(4260)/Y(4230)$, $P_c(4440), P_c(4457), P_c(4312), T_{cc}(3876)$, $X(6900)$
**	$\psi_2(3823), X(4140), X(4274)$, $X(4500), X(4700), Z_c(4360), Z_c(4430)$, $Z_{c1}(4050), Z_{c2}(4250), Z_c(4200), Z_c(4020)$ $Z_b(10610), Z_b(10650), Y(4660)$, $X(6200), X(7200)$ …
*	$Y(4008), Z_{cs}(3985), Z_{cs}(4000)$ ...

Why we do not see rich spectra arising from genuine color-singlet multiquark states?

2. Questions from the quark model: where are the genuine color-singlet multiquark states?

Heavy quarkonium spectrum *vs.* fully-heavy genuine color-singlet tetraquark states in the quark model

Hamiltonian in a non-relativistic quark model :

$$H = \left(\sum_{i=1}^{4} m_i + T_i\right) - T_G + \sum_{i<j} V_{ij}(r_{ij})$$

$$T_i = \frac{p_i^2}{2m_i}, \qquad V_{ij}(r_{ij}) = V_{ij}^{\mathrm{OGE}}(r_{ij}) + V_{ij}^{\mathrm{Conf}}(r_{ij}),$$

$$V_{ij}^{\mathrm{Conf}}(r_{ij}) = -\frac{3}{16}(\lambda_i \cdot \lambda_j) \cdot b r_{ij},$$

Potential smearing factor

$$V_{ij}^{\mathrm{OGE}} = \frac{\alpha_{ij}}{4}(\lambda_i \cdot \lambda_j)\left\{\frac{1}{r_{ij}} - \frac{\pi}{2} \cdot \frac{\sigma_{ij}^3 e^{-\sigma_{ij}^2 r_{ij}^2}}{\pi^{3/2}} \cdot \frac{4}{3 m_i m_j}(\boldsymbol{\sigma}_i \cdot \boldsymbol{\sigma}_j)\right\}$$

Coulomb

Spin-spin correl.

$$V_{ij}^{LS} = -\frac{\alpha_{ij}}{16}\frac{\lambda_i \cdot \lambda_j}{r_{ij}^3}\left(\frac{1}{m_i^2} + \frac{1}{m_j^2} + \frac{4}{m_i m_j}\right)\left\{\mathbf{L}_{ij} \cdot (\mathbf{S}_i + \mathbf{S}_j)\right\} - \frac{\alpha_{ij}}{16}\frac{\lambda_i \cdot \lambda_j}{r_{ij}^3}\left(\frac{1}{m_i^2} - \frac{1}{m_j^2}\right)\left\{\mathbf{L}_{ij} \cdot (\mathbf{S}_i - \mathbf{S}_j)\right\},$$

$$V_{ij}^{T} = -\frac{\alpha_{ij}}{4}(\lambda_i \cdot \lambda_j)\frac{1}{m_i m_j r_{ij}^3}\left\{\frac{3(\mathbf{S}_i \cdot \mathbf{r}_{ij})(\mathbf{S}_j \cdot \mathbf{r}_{ij})}{r_{ij}^2} - \mathbf{S}_i \cdot \mathbf{S}_j\right\}$$

- **Cornell model**
- **Godfrey-Isgur model**
- **A lot of recent development …**

Success of the Cornell model

$$V_{ij}(r_{ij}) = V_{ij}^{\mathrm{OGE}}(r_{ij}) + V_{ij}^{\mathrm{Conf}}(r_{ij})$$

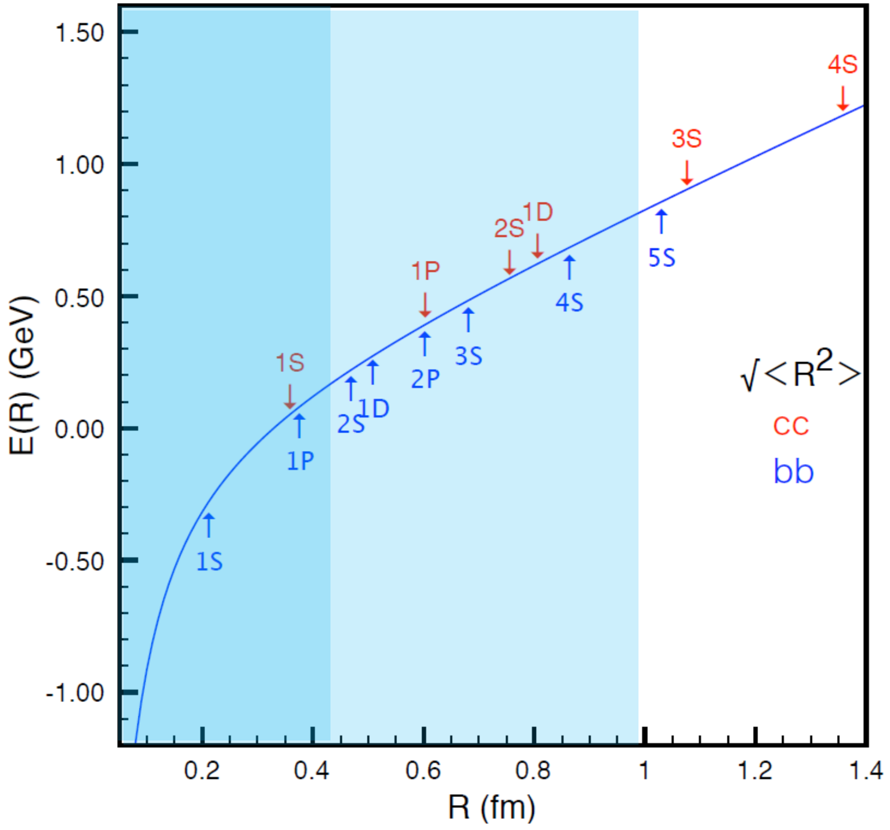

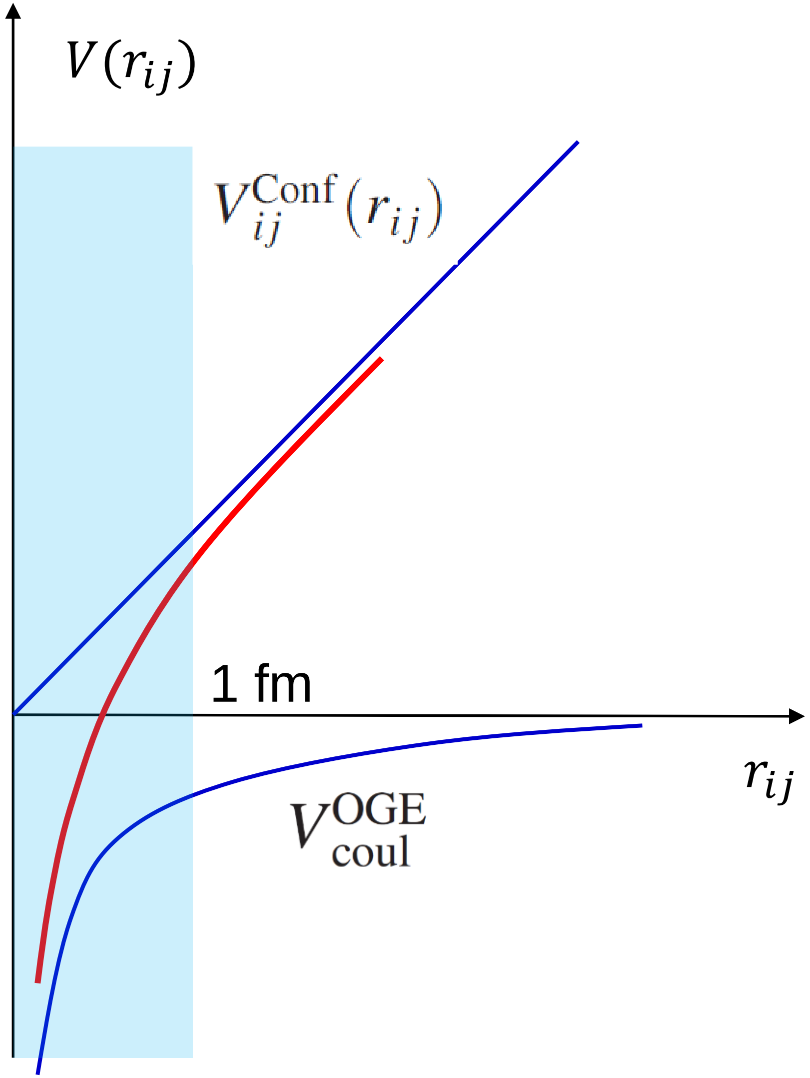

The size of most of those heavy quarkonia is less than 1 fm which indicate the dominance of the OGE potential.

The QM state $\chi_{c1}(2P)$ is about 60 MeV higher than the physical state $X(3872)$.

$n^{2S+1}L_J$	Name	J^{PC}	Exp. [6]	[8]	[11]	LP	SP
1^3S_1	J/ψ	1^{--}	3097[a]	3090	3097	3097	3097
1^1S_0	$\eta_c(1S)$	0^{-+}	2984[a]	2982	2979	2983	2984
2^3S_1	$\psi(2S)$	1^{--}	3686[a]	3672	3673	3679	3679
2^1S_0	$\eta_c(2S)$	0^{-+}	3639[a]	3630	3623	3635	3637
3^3S_1	$\psi(3S)$	1^{--}	4040[a]	4072	4022	4078	4030
3^1S_0	$\eta_c(3S)$	0^{-+}	...	4043	3991	4048	4004
4^3S_1	$\psi(4S)$	1^{--}	4415?	4406	4273	4412	4281
4^1S_0	$\eta_c(4S)$	0^{-+}	...	4384	4250	4388	4264
5^3S_1	$\psi(5S)$	1^{--}	...	...	4463	4711	4472
5^1S_0	$\eta_c(5S)$	0^{-+}	...	...	4446	4690	4459
1^3P_2	$\chi_{c2}(1P)$	2^{++}	3556[a]	3556	3554	3552	3553
1^3P_1	$\chi_{c1}(1P)$	1^{++}	3511[a]	3505	3510	3516	3521
1^3P_0	$\chi_{c0}(1P)$	0^{++}	3415[a]	3424	3433	3415	3415
1^1P_1	$h_c(1P)$	1^{+-}	3525[a]	3516	3519	3522	3526
2^3P_2	$\chi_{c2}(2P)$	2^{++}	3927[a]	3972	3937	3967	3937
2^3P_1	$\chi_{c1}(2P)$	1^{++}	...	3925	3901	3937	3914
2^3P_0	$\chi_{c0}(2P)$	0^{++}	3918?	3852	3842	3869	3848
2^1P_1	$h_c(2P)$	1^{+-}	...	3934	3908	3940	3916

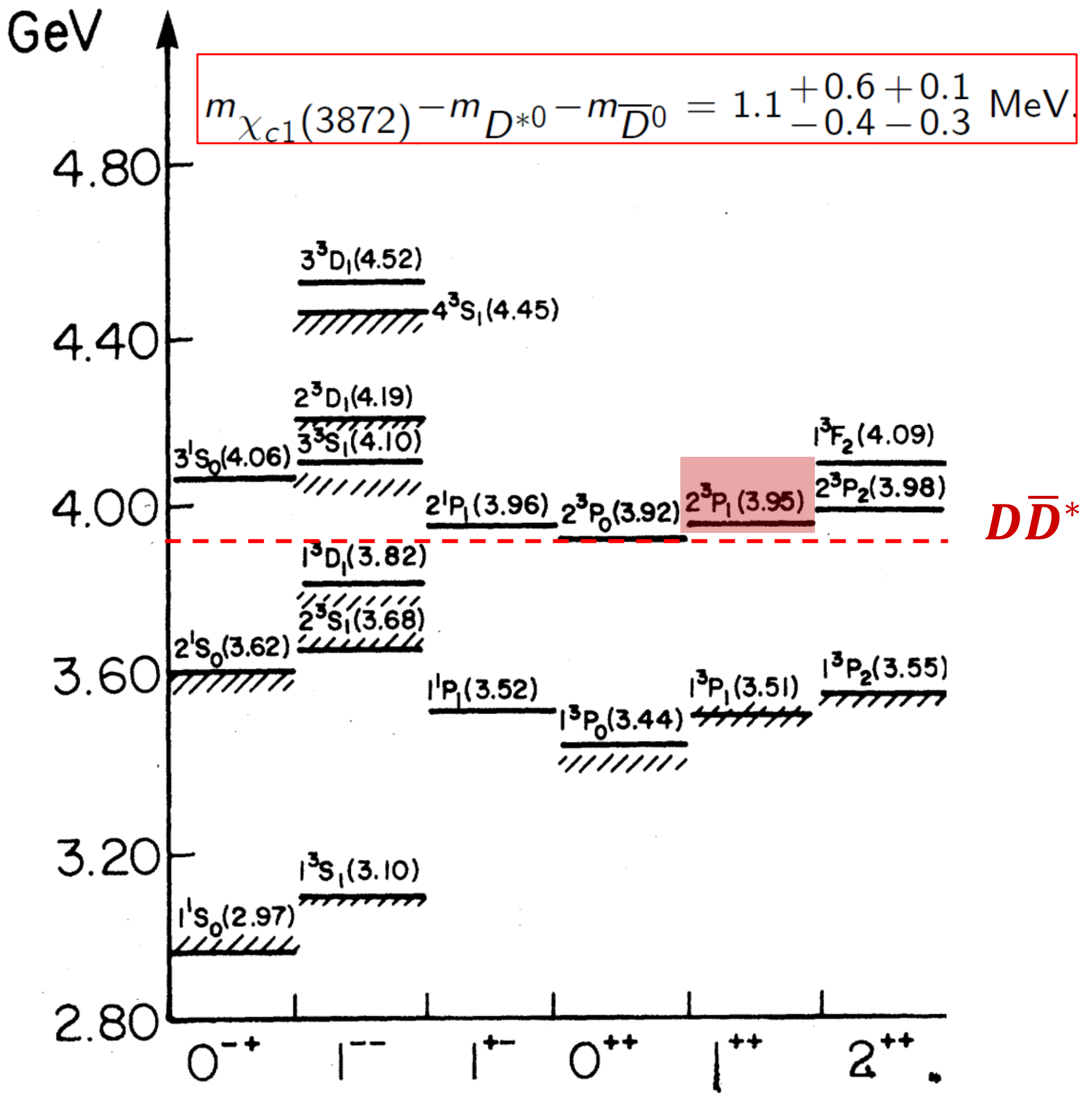

W.J. Deng et al., PRD95, 034026 (2017)

Godfrey and Isgur, PRD32, 189 (1985)

[8] T. Barnes, S. Godfrey, and E. S. Swanson, PRD 72, 054026 (2005).
[11] B. Q. Li and K. T. Chao, PRD 79, 094004 (2009).

When applied to multiquark systems, it's often argued that the linear confinement potential is a long-ranged dynamics. Thus, it can be neglected in heavy flavor system.

$$V_{ij}(r_{ij}) = V_{ij}^{\mathrm{OGE}}(r_{ij}) + V_{ij}^{\mathrm{Conf}}(r_{ij}) \simeq V_{ij}^{\mathrm{OGE}}(r_{ij})$$

For instance, the size of J/psi is about 0.4 fm and contributions from the confinement potential is relatively small and can be absorbed into the effective constituent quark mass. But for higher states, the confinement potential cannot be neglected.

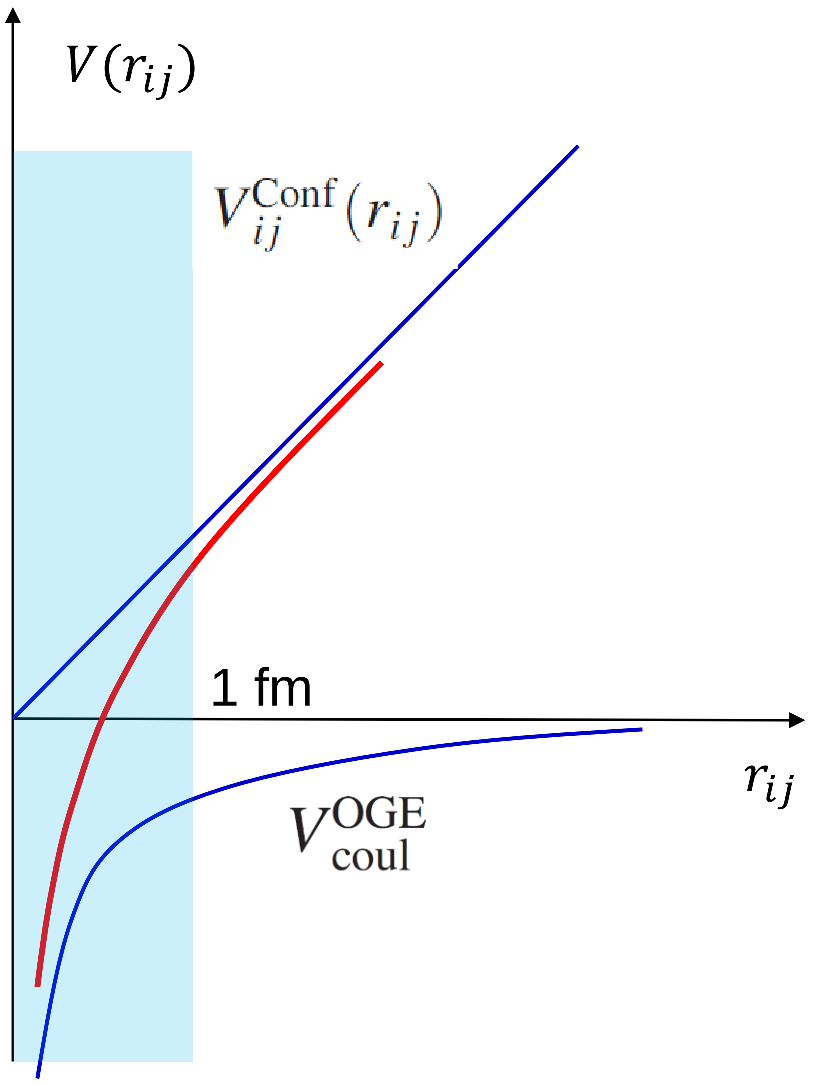

Energy decomposition of the low-lying charmonium states

	State	Mass	$\langle T\rangle$	$\langle V^{Lin}\rangle$	$\langle V^{Coul}\rangle$	$\langle V^{SS}\rangle$	$\langle V^{T}\rangle$	$\langle V^{LS}\rangle$
	1^1S_0	2984	523	232	-638	-100	...	...
J/ψ	1^3S_1	3097	379	267	-539	24	...	...
	2^1S_0	3635	451	554	-303	-33	...	...
$\psi(2S)$	2^3S_1	3679	426	572	-297	11	...	...
	1^3P_0	3417	555	383	-329	6	-115	-48
	1^1P_1	3522	375	456	-268	-7	...	...
	1^3P_1	3516	387	449	-272	3	-31	14
	1^3P_2	3552	328	485	-247	1	21	-2

For J/ψ, $\left|\frac{\langle V^{Lin}\rangle}{\langle V^{Coul}\rangle}\right| \simeq 0.49$

For $\psi(2S)$, $\left|\frac{\langle V^{Lin}\rangle}{\langle V^{Coul}\rangle}\right| \simeq 1.92$

The ratio increases quickly for excited states.

- The linear confinement potential increases with the excitation quantum numbers, while the Coulomb potential decreases. Their combined contribution drives the instability of the excited states.
- How do these energy terms evolve with the increased constituent degrees of freedom?

W.J. Deng, H. Liu, L.C. Gui, X.H. Zhong, PRD95, 034026 (2017)
M. S. Liu, Q. F. Lu, X. H. Zhong and Q. Zhao, PRD 100, 016006 (2019)

Fully-heavy tetraquarks as ideal exotic candidates

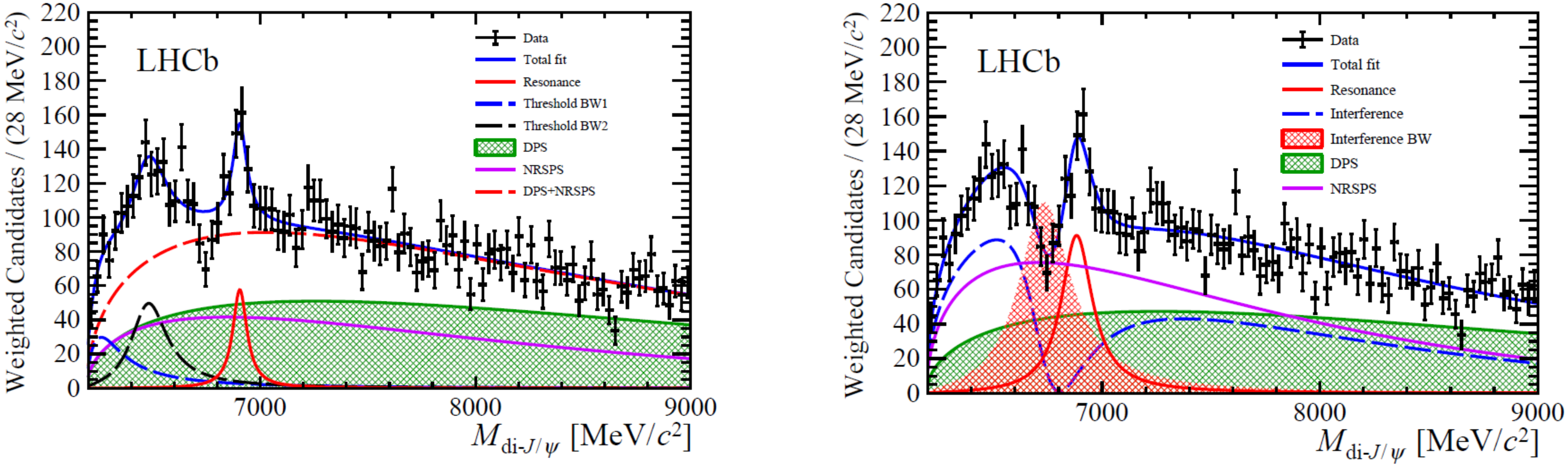

$m[X(6900)] = 6905 \pm 11 \pm 7\,\text{MeV}/c^2$

$\Gamma[X(6900)] = 80 \pm 19 \pm 33\,\text{MeV},$

$m[X(6900)] = 6886 \pm 11 \pm 11\,\text{MeV}/c^2$

$\Gamma[X(6900)] = 168 \pm 33 \pm 69\,\text{MeV}.$

LHCb Collaboration, arXiv:2006.16957v1 [hep-ex]

Unbound fully-heavy tetraquarks:

1. J.~P.~Ader, J.~M.~Richard and P.~Taxil, Phys.\ Rev.\ D {\bf 25}, 2370 (1982)
2. J.~M.~Richard, A.~Valcarce and J.~Vijande, Phys.\ Rev.\ D {\bf 95}, 054019 (2017); Phys.\ Rev.\ C {\bf 97}, 035211 (2018)
3. M.~Karliner, S.~Nussinov and J.~L.~Rosner, Phys.\ Rev.\ D {\bf 95}, 034011 (2017)
4. J.~Wu, Y.~R.~Liu, K.~Chen, X.~Liu, and S.~L.~Zhu, Phys.\ Rev.\ D {\bf 97}, 094015 (2018)
5. M. S. Liu, Q. F. Lu, X. H. Zhong and Q. Zhao, Phys. Rev. D 100, 016006 (2019).
6. M.S. Liu, F.X. Liu, X.H. Zhong and Q. Zhao, 2006.11952 [hep-ph].
7. X.Z. Weng, X.L. Chen, W.Z. Deng, and S.L. Zhu, arXiv:2010.05163v1 [hep-ph]

Bound fully-heavy tetraquarks:

1. L.~Heller and J.~A.~Tjon, Phys.\ Rev.\ D {\bf 32}, 755 (1985)
2. R.~J.~Lloyd and J.~P.~Vary, Phys.\ Rev.\ D {\bf 70}, 014009 (2004)
3. N.~Barnea, J.~Vijande and A.~Valcarce, Phys.\ Rev.\ D {\bf 73}, 054004 (2006);
4. M.~N.~Anwar, J.~Ferretti, F.~K.~Guo, E.~Santopinto and B.~S.~Zou, Eur.\ Phys.\ J.\ C {\bf 78}, 647 (2018)
5. Y.~Bai, S.~Lu and J.~Osborne, Phys.Lett.B 798 (2019) 134930

CMS-PAS-BPH-21-003

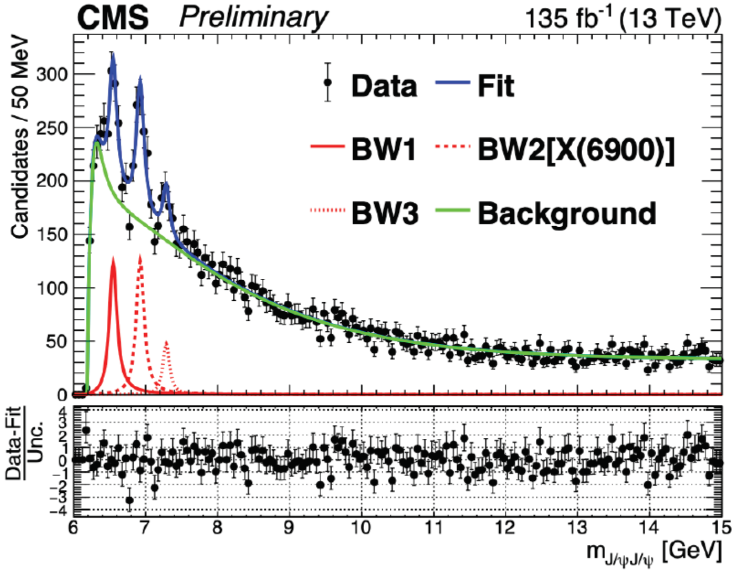

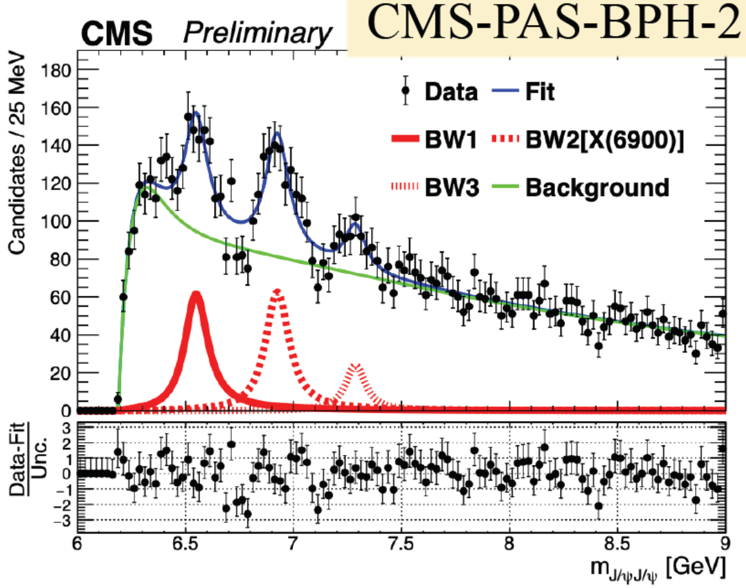

ATLAS-CONF-2022- 040

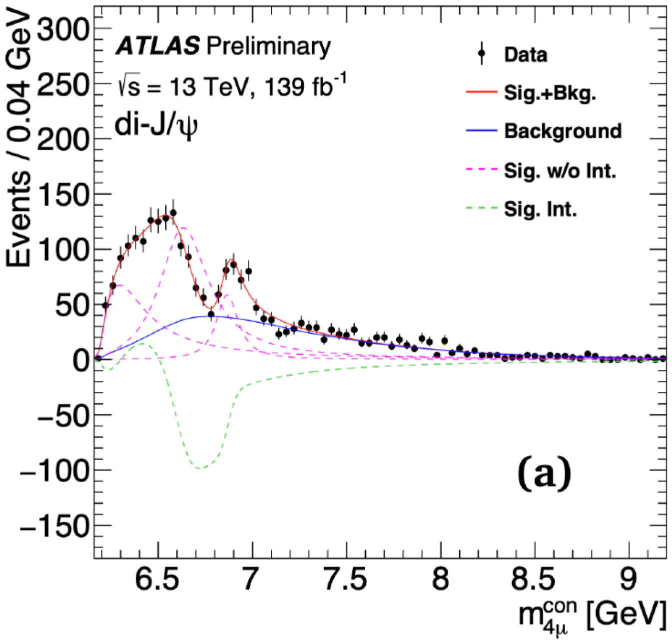

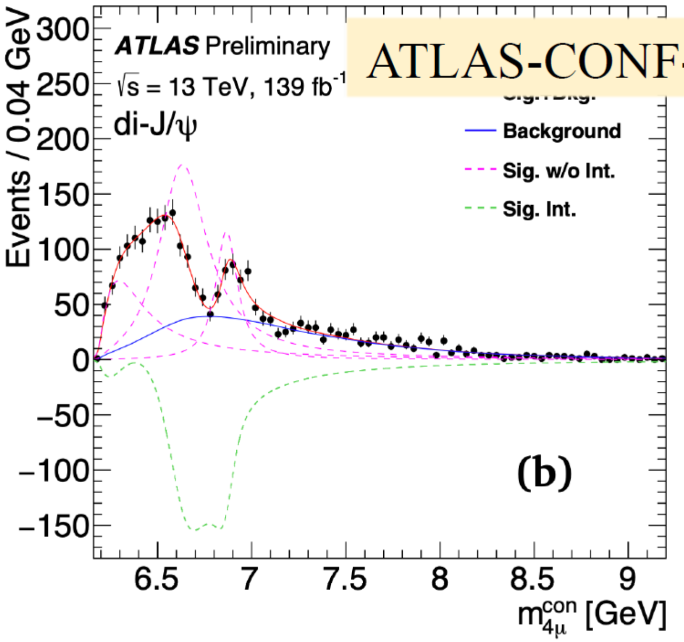

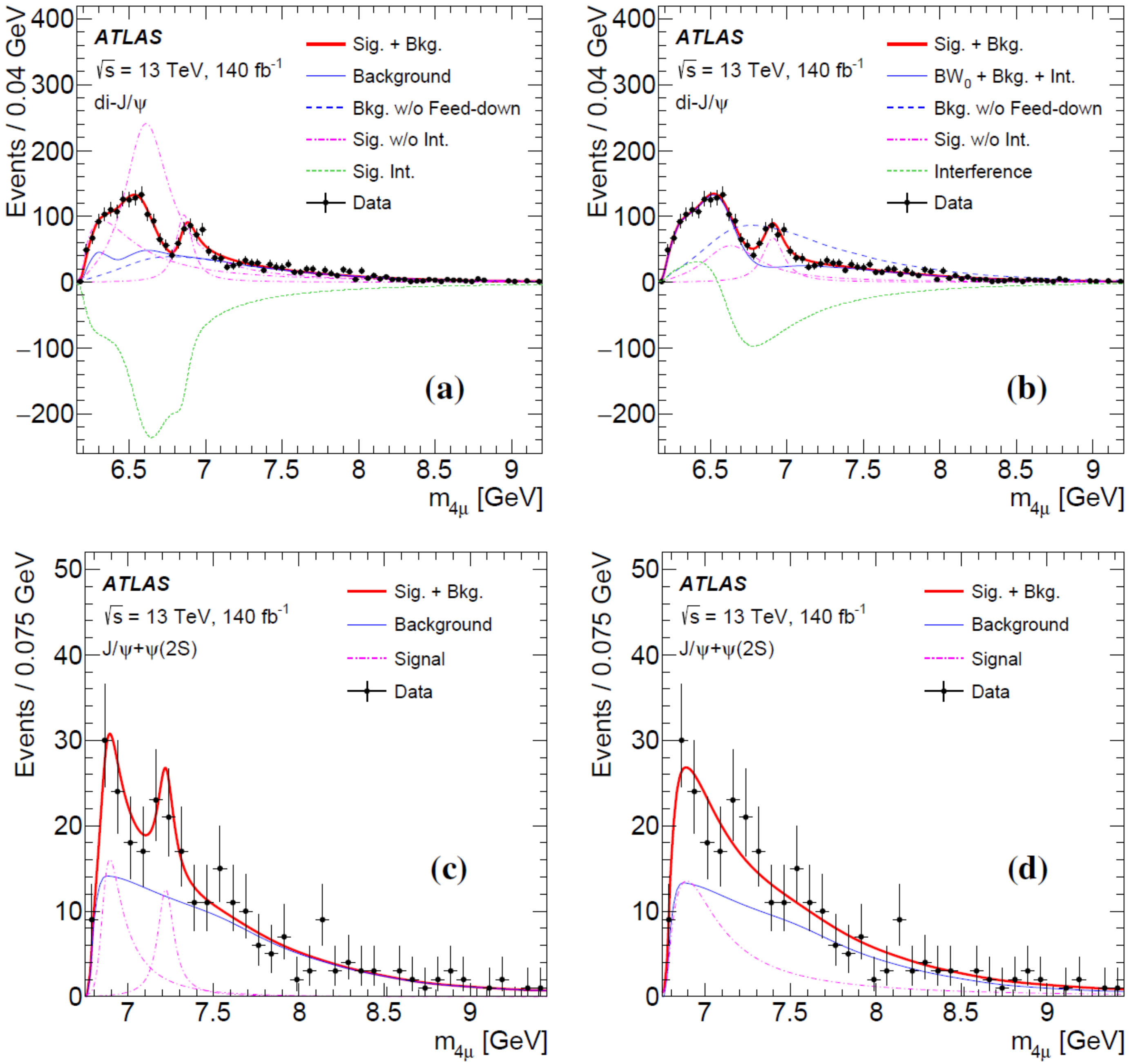

di-J/ψ

J/ψ-$\psi(2S)$

ATLAS Colla., arXiv:2304.08962v1 [hep-ex]

Constituent quark models:

X. Jin et al., Eur.Phys.J.C 80 (2020) 11, 1083
G. Yang, J.L. Ping, J. Segovia, Symmetry 12 (2020) 11, 1869
X.Z. Wen et al., Phys.Rev.D 103 (2021) 3, 034001 [only the color-magnetic interaction included]
Q.F. Lyu et al., Eur.Phys.J.C 80 (2020) 9, 871 [Extended relativized quark model]
M.C. Gordillo, F. De. Soto, J. Segovia, Phys.Rev.D 102 (2020) 11, 114007 [Difussion Monto Carlo mechod]
M.S. Liu, F.X. Liu, X.H. Zhong, Q. Zhao, 2006.11952 [hep-ph]
F.X. Liu, M.S. Liu, X.H. Zhong, and Q. Zhao, PRD 104, 116029 (2021)
G.J. Wang, L. Meng, M. Oka, S.L. Zhu, PRD 104, 036016 (2021)
J. Hu, B.R. He, and J.L. Ping, Eur.Phys.J.C 83 (2023) 7, 559

Coupled-channel approach:

X.K. Dong, V. Baru, C. Hanhart, F.K. Guo, A. Nefediev, Phys.Rev.Lett. 126 (2021) 13, 132001
C. Gong, M.C. Du, Q. Zhao, X.H. Zhong, B. Zhou, Phys.Lett.B 824 (2022) 136794
Z. Zhang et al., Phys.Rev.D 105 (2022) 5, 054026
Z.H. Guo, J.A. Oller, Phys.Rev.D 103 (2021) 3, 034024
C. Gong, M.C. Du, Q. Zhao, Phys.Rev.D 106 (2022), 054011

Diquark model:

M.A. Bedolla et al., Eur.Phys.J.C 80 (2020) 11, 1004
J.F. Giron, R.F. Lebed, Phys.Rev.D 102 (2020) 7, 074003
M. Karliner, J.L. Rosner, Phys.Rev.D 102 (2020) 11, 114039
R.N. Faustov, et al., Universe 7 (2021) 4, 94
H.W. Ke, X.H. Liu, Y.L. Shi, Eur.Phys.J.C 81 (2021) 5, 427

Hybrid tetraquark:

L.B. Wang and C.F. Qiao, Phys.Lett.B 817 (2021) 136339

QCD sum rules:

Z.G. Wang, Int.J.Mod.Phys.A 36 (2021) 02, 2150014
Q.N. Wang, Z.Y. Yang, W. Chen, Phys.Rev.D 104 (2021) 11, 114037
R.H. Wu et al., JHEP 11 (2022) 023

Production and decay mechanisms:

C. Becchi, A. Giachino, L. Maiani, E. Santopinto, Phys.Lett.B 811 (2020) 135952
J.Z. Wang, D.Y. Chen, X. Liu, T. Matsuki, Phys.Rev.D 103 (2021) 7, 071503
R.L. Zhu, Nucl.Phys.B 966 (2021) 115393
Rafał Maciuła et al., Phys.Lett.B 812 (2021) 136010
Y.Q. Ma and H.F. Zhang, 2009.08376 [hep-ph]
F. Feng et al., Phys.Rev.D 106 (2022) 11, 114029
V. P. Gonçalves, Bruno D. Moreira, Phys.Lett.B 816 (2021) 136249

Now, all the calculated masses are above the di-charmonium threshold!

Typical fully-heavy tetraquark system with color-spin-flavor symmetry

$T = Q_1 Q_2 \bar{Q}_3 \bar{Q}_4 \ (cc\bar{c}\bar{c}, bb\bar{b}\bar{b}, cc\bar{b}\bar{b}, bc\bar{b}\bar{c}, bc\bar{c}\bar{c}, bc\bar{b}\bar{b}, \ldots)$

– ideal candidates for genuine tetraquark states

Stability of the four-body system:

$M_T < 4m_Q$ → stable

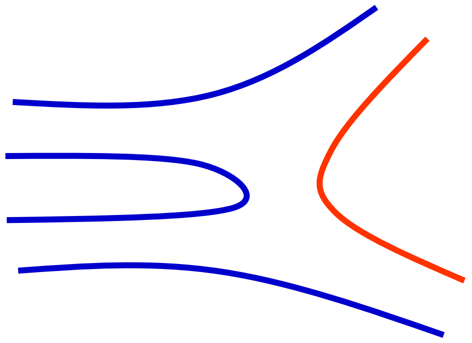

$M_T > 4m_Q$ → unstable.

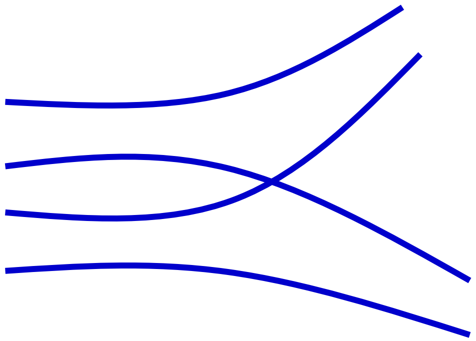

Typical fully-heavy tetraquark system with color-spin-flavor symmetry

$T = Q_1 Q_2 \bar{Q}_3 \bar{Q}_4$ $(cc\bar{c}\bar{c}, bb\bar{b}\bar{b}, cc\bar{b}\bar{b}, bc\bar{b}\bar{c}, bc\bar{c}\bar{c}, bc\bar{b}\bar{b}, \ldots)$

Diquark (anti-diquark) configurations:

- Spin: $2 \otimes 2 = 1 + 4$
- Color: $3 \otimes 3 = \bar{3} + 6$; $\bar{3} \otimes \bar{3} = 3 + \bar{6}$
- Flavor: $\{Q_1 Q_2\} = (Q_1 Q_2 + Q_2 Q_1)/\sqrt{2}$; $[Q_1 Q_2] = (Q_1 Q_2 - Q_2 Q_1)/\sqrt{2}$

$$
\begin{cases}
|1\rangle = |[Q_1 Q_2]_1^6 [\bar{Q}_3 \bar{Q}_4]_1^{\bar{6}}\rangle_0^0, & |2\rangle = |\{Q_1 Q_2\}_0^6 \{\bar{Q}_3 \bar{Q}_4\}_0^{\bar{6}}\rangle_0^0, \\
|3\rangle = |\{Q_1 Q_2\}_1^{\bar{3}} \{\bar{Q}_3 \bar{Q}_4\}_1^{3}\rangle_0^0, & |4\rangle = |[Q_1 Q_2]_0^{\bar{3}} [\bar{Q}_3 \bar{Q}_4]_0^{3}\rangle_0^0, \\
|5\rangle = |[Q_1 Q_2]_1^6 [\bar{Q}_3 \bar{Q}_4]_1^{\bar{6}}\rangle_1^0, & |6\rangle = |[Q_1 Q_2]_1^6 \{\bar{Q}_3 \bar{Q}_4\}_0^{\bar{6}}\rangle_1^0, \\
|7\rangle = |\{Q_1 Q_2\}_0^6 [\bar{Q}_3 \bar{Q}_4]_1^{\bar{6}}\rangle_1^0, & |8\rangle = |\{Q_1 Q_2\}_1^{\bar{3}} \{\bar{Q}_3 \bar{Q}_4\}_1^{3}\rangle_1^0, \\
|9\rangle = |\{Q_1 Q_2\}_1^{\bar{3}} [\bar{Q}_3 \bar{Q}_4]_0^{3}\rangle_1^0, & |10\rangle = |[Q_1 Q_2]_0^{\bar{3}} \{\bar{Q}_3 \bar{Q}_4\}_1^{3}\rangle_1^0, \\
|11\rangle = |[Q_1 Q_2]_1^6 [\bar{Q}_3 \bar{Q}_4]_1^{\bar{6}}\rangle_2^0, & |12\rangle = |\{Q_1 Q_2\}_1^{\bar{3}} \{\bar{Q}_3 \bar{Q}_4\}_1^{3}\rangle_2^0,
\end{cases}
$$

TABLE I. Configurations of all-heavy tetraquarks.

System	$J^{P(C)}$	Configuration		
$cc\bar{c}\bar{c}$	0^{++}	$\vert\{cc\}^6_0\{\bar{c}\bar{c}\}^{\bar{6}}_0\rangle^0_0$	$\vert\{cc\}^{\bar{3}}_1\{\bar{c}\bar{c}\}^3_1\rangle^0_0$	$\cdots$
	1^{+-}	$\vert\{cc\}^{\bar{3}}_1\{\bar{c}\bar{c}\}^3_1\rangle^0_1$	$\cdots$	$\cdots$
	2^{++}	$\vert\{cc\}^{\bar{3}}_1\{\bar{c}\bar{c}\}^3_1\rangle^0_2$	$\cdots$	$\cdots$
$bb\bar{b}\bar{b}$	0^{++}	$\vert\{bb\}^6_0\{\bar{b}\bar{b}\}^{\bar{6}}_0\rangle^0_0$	$\vert\{bb\}^{\bar{3}}_1\{\bar{b}\bar{b}\}^3_1\rangle^0_0$	$\cdots$
	1^{+-}	$\vert\{bb\}^{\bar{3}}_1\{\bar{b}\bar{b}\}^3_1\rangle^0_1$	$\cdots$	$\cdots$
	2^{++}	$\vert\{bb\}^{\bar{3}}_1\{\bar{b}\bar{b}\}^3_1\rangle^0_2$	$\cdots$	$\cdots$
$bb\bar{c}\bar{c}$	0^{+}	$\vert\{bb\}^6_0\{\bar{c}\bar{c}\}^{\bar{6}}_0\rangle^0_0$	$\vert\{bb\}^{\bar{3}}_1\{\bar{c}\bar{c}\}^3_1\rangle^0_0$	$\cdots$
	1^{+}	$\vert\{bb\}^{\bar{3}}_1\{\bar{c}\bar{c}\}^3_1\rangle^0_1$	$\cdots$	$\cdots$
	2^{+}	$\vert\{bb\}^{\bar{3}}_1\{\bar{c}\bar{c}\}^3_1\rangle^0_2$	$\cdots$	$\cdots$
$bc\bar{c}\bar{c}$	0^{+}	$\vert(bc)^6_0\{\bar{c}\bar{c}\}^{\bar{6}}_0\rangle^0_0$	$\vert(bc)^{\bar{3}}_1\{\bar{c}\bar{c}\}^3_1\rangle^0_0$	$\cdots$
	1^{+}	$\vert(bc)^6_1\{\bar{c}\bar{c}\}^{\bar{6}}_0\rangle^0_1$	$\vert(bc)^{\bar{3}}_1\{\bar{c}\bar{c}\}^3_1\rangle^0_1$	$\vert(bc)^{\bar{3}}_0\{\bar{c}\bar{c}\}^3_1\rangle^0_1$
	2^{+}	$\vert(bc)^{\bar{3}}_1\{\bar{c}\bar{c}\}^3_1\rangle^0_2$	$\cdots$	$\cdots$
$bc\bar{b}\bar{b}$	0^{+}	$\vert(bc)^6_0\{\bar{b}\bar{b}\}^{\bar{6}}_0\rangle^0_0$	$\vert(bc)^{\bar{3}}_1\{\bar{b}\bar{b}\}^3_1\rangle^0_0$	$\cdots$
	1^{+}	$\vert(bc)^6_1\{\bar{b}\bar{b}\}^{\bar{6}}_0\rangle^0_1$	$\vert(bc)^{\bar{3}}_1\{\bar{b}\bar{b}\}^3_1\rangle^0_1$	$\vert(bc)^{\bar{3}}_0\{\bar{b}\bar{b}\}^3_1\rangle^0_1$
	2^{+}	$\vert(bc)^{\bar{3}}_1\{\bar{b}\bar{b}\}^3_1\rangle^0_2$	$\cdots$	$\cdots$
$bc\bar{b}\bar{c}$	0^{++}	$\vert(bc)^6_1(\bar{b}\bar{c})^{\bar{6}}_1\rangle^0_0$	$\vert(bc)^6_0(\bar{b}\bar{c})^{\bar{6}}_0\rangle^0_0$	$\cdots$
		$\vert(bc)^{\bar{3}}_1(\bar{b}\bar{c})^3_1\rangle^0_0$	$\vert(bc)^{\bar{3}}_0(\bar{b}\bar{c})^3_0\rangle^0_0$	$\cdots$
	1^{+-}	$\vert(bc)^6_1(\bar{b}\bar{c})^{\bar{6}}_1\rangle^0_1$	$\frac{1}{\sqrt{2}}\vert(bc)^6_1(\bar{b}\bar{c})^{\bar{6}}_0\rangle^0_1 - \vert(bc)^6_0(\bar{b}\bar{c})^{\bar{6}}_1\rangle^0_1$	$\cdots$
		$\vert(bc)^{\bar{3}}_1(\bar{b}\bar{c})^3_1\rangle^0_1$	$\frac{1}{\sqrt{2}}\vert(bc)^{\bar{3}}_1(\bar{b}\bar{c})^3_0\rangle^0_1 - \vert(bc)^{\bar{3}}_0(\bar{b}\bar{c})^3_1\rangle^0_1$	$\cdots$
	1^{++}	$\frac{1}{\sqrt{2}}\vert(bc)^6_1(\bar{b}\bar{c})^{\bar{6}}_0\rangle^0_1 + \vert(bc)^6_0(\bar{b}\bar{c})^{\bar{6}}_1\rangle^0_1$	$\frac{1}{\sqrt{2}}\vert(bc)^{\bar{3}}_1(\bar{b}\bar{c})^3_0\rangle^0_1 + \vert(bc)^{\bar{3}}_0(\bar{b}\bar{c})^3_1\rangle^0_1$	$\cdots$
	2^{++}	$\vert(bc)^6_1(\bar{b}\bar{c})^{\bar{6}}_1\rangle^0_2$	$\vert(bc)^{\bar{3}}_1(\bar{b}\bar{c})^3_1\rangle^0_2$	$\cdots$

Reminder of the Hamiltonian adopted

Hamiltonian in a non-relativistic quark model:

$$H = \left(\sum_{i=1}^{4} m_i + T_i\right) - T_G + \sum_{i<j} V_{ij}(r_{ij})$$

$$\begin{cases} T_i = \dfrac{p_i^2}{2m_i} \\ V_{ij}(r_{ij}) = V_{ij}^{\mathrm{OGE}}(r_{ij}) + V_{ij}^{\mathrm{Conf}}(r_{ij}), \\ V_{ij}^{\mathrm{Conf}}(r_{ij}) = -\dfrac{3}{16}(\boldsymbol{\lambda}_i \cdot \boldsymbol{\lambda}_j) \cdot b r_{ij}, \\ V_{ij}^{\mathrm{OGE}} = \dfrac{\alpha_{ij}}{4}(\boldsymbol{\lambda}_i \cdot \boldsymbol{\lambda}_j)\left\{\dfrac{1}{r_{ij}} - \dfrac{\pi}{2} \cdot \dfrac{\sigma_{ij}^3 e^{-\sigma_{ij}^2 r_{ij}^2}}{\pi^{3/2}} \cdot \dfrac{4}{3m_i m_j}(\boldsymbol{\sigma}_i \cdot \boldsymbol{\sigma}_j)\right\} \end{cases}$$

$$\begin{cases} V_{ij}^{LS} = -\dfrac{\alpha_{ij}}{16}\dfrac{\boldsymbol{\lambda}_i \cdot \boldsymbol{\lambda}_j}{r_{ij}^3}\left(\dfrac{1}{m_i^2} + \dfrac{1}{m_j^2} + \dfrac{4}{m_i m_j}\right)\left\{\mathbf{L}_{ij} \cdot (\mathbf{S}_i + \mathbf{S}_j)\right\} \\ \qquad - \dfrac{\alpha_{ij}}{16}\dfrac{\boldsymbol{\lambda}_i \cdot \boldsymbol{\lambda}_j}{r_{ij}^3}\left(\dfrac{1}{m_i^2} - \dfrac{1}{m_j^2}\right)\left\{\mathbf{L}_{ij} \cdot (\mathbf{S}_i - \mathbf{S}_j)\right\}, \\ V_{ij}^{T} = -\dfrac{\alpha_{ij}}{4}(\boldsymbol{\lambda}_i \cdot \boldsymbol{\lambda}_j)\dfrac{1}{m_i m_j r_{ij}^3}\left\{\dfrac{3(\mathbf{S}_i \cdot \mathbf{r}_{ij})(\mathbf{S}_j \cdot \mathbf{r}_{ij})}{r_{ij}^2} - \mathbf{S}_i \cdot \mathbf{S}_j\right\} \end{cases}$$

Color matrix elements:

	$\langle\boldsymbol{\lambda}_1 \cdot \boldsymbol{\lambda}_2\rangle$	$\langle\boldsymbol{\lambda}_3 \cdot \boldsymbol{\lambda}_4\rangle$	$\langle\boldsymbol{\lambda}_1 \cdot \boldsymbol{\lambda}_3\rangle$	$\langle\boldsymbol{\lambda}_2 \cdot \boldsymbol{\lambda}_4\rangle$	$\langle\boldsymbol{\lambda}_1 \cdot \boldsymbol{\lambda}_4\rangle$	$\langle\boldsymbol{\lambda}_2 \cdot \boldsymbol{\lambda}_3\rangle$
$\langle\zeta_1\|\hat{O}\|\zeta_1\rangle$	$4/3$	$4/3$	$-10/3$	$-10/3$	$-10/3$	$-10/3$
$\langle\zeta_2\|\hat{O}\|\zeta_2\rangle$	$-8/3$	$-8/3$	$-4/3$	$-4/3$	$-4/3$	$-4/3$
$\langle\zeta_1\|\hat{O}\|\zeta_2\rangle$	0	0	$-2\sqrt{2}$	$-2\sqrt{2}$	$2\sqrt{2}$	$2\sqrt{2}$

$$\begin{cases} \zeta_1 = |6\bar{6}\rangle = |(Q_1Q_2)^6(\bar{Q}_3\bar{Q}_4)^{\bar{6}}\rangle^0 \\ \zeta_2 = |\bar{3}3\rangle = |(Q_1Q_2)^{\bar{3}}(\bar{Q}_3\bar{Q}_4)^{3}\rangle^0 \end{cases}$$

Dynamic feature for fully-heavy tetraquark system

Jacobi coordinates:

$$
\begin{cases}
\boldsymbol{\xi}_1 \equiv \mathbf{r}_1 - \mathbf{r}_2, \\
\boldsymbol{\xi}_2 \equiv \mathbf{r}_3 - \mathbf{r}_4, \\
\boldsymbol{\xi}_3 \equiv \dfrac{m_1\mathbf{r}_1 + m_2\mathbf{r}_2}{m_1 + m_2} - \dfrac{m_3\mathbf{r}_3 + m_4\mathbf{r}_4}{m_3 + m_4}, \\
\boldsymbol{\xi}_4 \equiv \dfrac{m_1\mathbf{r}_1 + m_2\mathbf{r}_2 + m_3\mathbf{r}_3 + m_4\mathbf{r}_4}{m_1 + m_2 + m_3 + m_4},
\end{cases}
$$

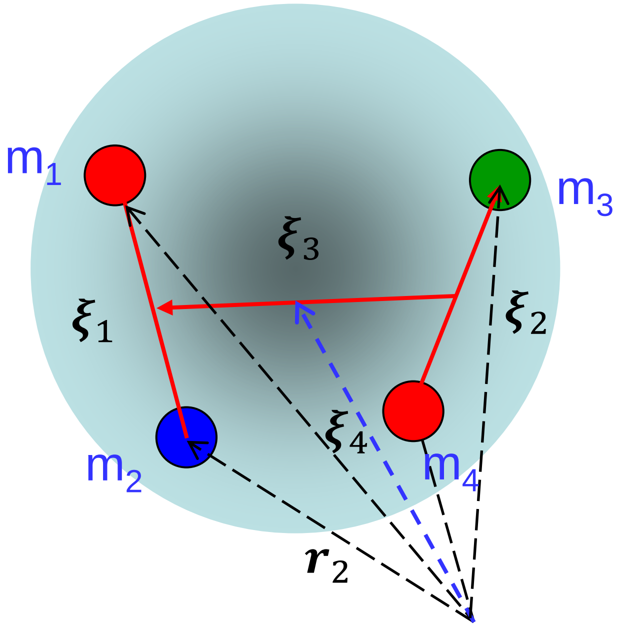

Jacobi coordinate

Trial wavefunction for the ground states expanded by a series of Gaussian functions:

$$\psi(\mathbf{r}_1, \mathbf{r}_2, \mathbf{r}_3, \mathbf{r}_4) = \sum_{\ell}^{n} C_\ell \prod_{i=1}^{4} \left(\frac{m_i\omega_\ell}{\pi}\right)^{3/4} \exp\left[-\frac{m_i\omega_\ell}{2} r_i^2\right]$$

$$\Rightarrow \quad \psi(\xi_1, \xi_2, \xi_3, \xi_4) = \sum_{\ell}^{n} C_\ell \prod_{i=1}^{4} \left(\frac{\mu_i\omega_\ell}{\pi}\right)^{3/4} \exp\left[-\frac{\mu_i\omega_\ell}{2} \xi_i^2\right]$$

E. Hiyama, Y. Kino, and M. Kamimura, Gaussian expansion method for few-body systems, Prog. Part. Nucl. Phys. 51, 223 (2003).
M. S. Liu, Q. F. Lu, X. H. Zhong and Q. Zhao, PRD 100, 016006 (2019).
M.S. Liu, F.X. Liu, X.H. Zhong and Q. Zhao, 2006.11952 [hep-ph], PRD 109, 076017 (2024).

The contributions from each part of the Hamiltonian of the $cc\bar{c}\bar{c}$ and $bb\bar{b}\bar{b}$ systems in units of MeV with $L = 0$.

J^{PC}	Configuration	M	$\langle T \rangle$	$\langle V^{\text{Conf}} \rangle$	$\langle V^{\text{OGE}}_{\text{coul}} \rangle$	$\langle V^{\text{OGE}}_{CM} \rangle$
0^{++}	$\lvert \{cc\}^6_0 \{\bar{c}\bar{c}\}^{\bar{6}}_0 \rangle^0_0$	6518	715	664	−811	18
	$\lvert \{cc\}^{\bar{3}}_1 \{\bar{c}\bar{c}\}^3_1 \rangle^0_0$	6487	756	646	−834	−13
1^{+-}	$\lvert \{cc\}^{\bar{3}}_1 \{\bar{c}\bar{c}\}^3_1 \rangle^0_1$	6500	739	653	−825	0
2^{++}	$\lvert \{cc\}^{\bar{3}}_1 \{\bar{c}\bar{c}\}^3_1 \rangle^0_2$	6524	708	667	−806	23
0^{++}	$\lvert \{bb\}^6_0 \{\bar{b}\bar{b}\}^{\bar{6}}_0 \rangle^0_0$	19338	768	356	−1203	9
	$\lvert \{bb\}^{\bar{3}}_1 \{\bar{b}\bar{b}\}^3_1 \rangle^0_0$	19322	796	350	−1225	−6
1^{+-}	$\lvert \{bb\}^{\bar{3}}_1 \{\bar{b}\bar{b}\}^3_1 \rangle^0_1$	19329	785	353	−1216	0
2^{++}	$\lvert \{bb\}^{\bar{3}}_1 \{\bar{b}\bar{b}\}^3_1 \rangle^0_2$	19341	763	357	−1199	12

- The confining potential contributes a positive energy and cannot be neglected.
- This implies that the four-quark systems are located above the two-heavy meson thresholds.
- The treatment of the confinement potential seems to distinguish models in the literature.

(M. S. Liu, Q. F. Lu, X. H. Zhong and Q. Zhao, Phys. Rev. D 100, 016006 (2019).)

Predicted masses (MeV) for the $cc\bar{c}\bar{c}$ system compared with other models.

State	Ours	Ref. [29]	Ref. [16]	Ref. [11]	Ref. [12]	Ref. [13]	Ref. [22]	Ref. [17]	Refs. [25,26]	Ref. [27]	Ref. [24]	Ref. [21]
0^{++}	6487	6797	6477	6460–6470	6437	6200	6192	6038–6115	5990	5969	5966	<6140
0^{++}	6518	7016	6695	6440–6820	6383	…	…	…	…	…	…	
1^{+-}	6500	6899	6528	6370–6510	6437	…	…	6101–6176	6050	6021	6051	
2^{++}	6524	6956	6573	6370–6510	6437	…	…	6172–6216	6090	6115	6223	

TABLE VIII. Our predicted masses (MeV) for the $bb\bar{b}\bar{b}$ system compared with others.

State	Ours	Ref. [29]	Refs. [25,26]	Ref. [22]	Ref. [24]	Ref. [21]	Ref. [23]	Ref. [11]	Ref. [30]	Ref. [21]
0^{++}	19322	20155	18840	18826	18754	18720	18690	18460–18490	18798	<18890
0^{++}	19338	20275	⋯	⋯	⋯	⋯	⋯	18450–19640	⋯	
1^{+-}	19329	20212	18840	⋯	18808	⋯	⋯	18320–18540	⋯	
2^{++}	19341	20243	18850	⋯	18916	⋯	⋯	18320–18530	⋯	

[11] W. Chen, H. X. Chen, X. Liu, T. G. Steele, and S. L. Zhu, Phys. Lett. B 773, 247 (2017).
[12] J. P. Ader, J.M. Richard, and P. Taxil, Phys. Rev. D 25, 2370 (1982),
[13] Y. Iwasaki, Prog. Theor. Phys. 54, 492 (1975)
[16] R. J. Lloyd and J. P. Vary, Phys. Rev. D 70, 014009 (2004)
[17] N. Barnea, J. Vijande, and A. Valcarce, Phys. Rev. D73, 054004 (2006).
[21] M. N. Anwar, J. Ferretti, F. K. Guo, E. Santopinto, and B. S. Zou, Eur. Phys. J. C 78, 647 (2018).
[22] M. Karliner, S. Nussinov, and J. L. Rosner, Phys. Rev. D 95, 034011 (2017).
[23] Y. Bai, S. Lu, and J. Osborne, arXiv:1612.00012.
[24] A. V. Berezhnoy, A. V. Luchinsky, and A. A. Novoselov, Phys. Rev. D 86, 034004 (2012).
[25] Z. G. Wang, Eur. Phys. J. C 77, 432 (2017).
[26] Z. G. Wang and Z. Y. Di, arXiv:1807.08520.
[27] V. R. Debastiani and F. S. Navarra, Chin. Phys. C 43, 013105 (2019).
[29] J. Wu, Y. R. Liu, K. Chen, X. Liu, and S. L. Zhu, Phys. Rev. D 97, 094015 (2018).
[30] C. Hughes, E. Eichten, and C. T. H. Davies, Phys. Rev. D 97, 054505 (2018).

Predicted mass spectra for the $cc\bar{c}\bar{c}$, $bb\bar{b}\bar{b}$ and $bb\bar{c}\bar{c}$ systems.

$J^{P(C)}$	Configuration	$\langle H \rangle$ (MeV)
0^{++}	$\|\{cc\}^{6}_{0}\{\bar{c}\,\bar{c}\}^{\bar{6}}_{0}\rangle^{0}_{0}$	$\begin{pmatrix} 6518 & -0.2371 \\ -0.2371 & 6487 \end{pmatrix}$
	$\|\{cc\}^{\bar{3}}_{1}\{\bar{c}\,\bar{c}\}^{3}_{1}\rangle^{0}_{0}$	
1^{+-}	$\|\{cc\}^{\bar{3}}_{1}\{\bar{c}\,\bar{c}\}^{3}_{1}\rangle^{0}_{1}$	(6500)
2^{++}	$\|\{cc\}^{\bar{3}}_{1}\{\bar{c}\,\bar{c}\}^{3}_{1}\rangle^{0}_{2}$	(6524)
0^{++}	$\|\{bb\}^{6}_{0}\{\bar{b}\,\bar{b}\}^{\bar{6}}_{0}\rangle^{0}_{0}$	$\begin{pmatrix} 19338 & -0.1102 \\ -0.1102 & 19322 \end{pmatrix}$
	$\|\{bb\}^{\bar{3}}_{1}\{\bar{b}\,\bar{b}\}^{3}_{1}\rangle^{0}_{0}$	
1^{+-}	$\|\{bb\}^{\bar{3}}_{1}\{\bar{b}\,\bar{b}\}^{3}_{1}\rangle^{0}_{1}$	(19329)
2^{++}	$\|\{bb\}^{\bar{3}}_{1}\{\bar{b}\,\bar{b}\}^{3}_{1}\rangle^{0}_{2}$	(19341)
0^{+}	$\|\{bb\}^{6}_{0}\{\bar{c}\,\bar{c}\}^{\bar{6}}_{0}\rangle^{0}_{0}$	$\begin{pmatrix} 13032 & -0.1105 \\ -0.1105 & 12953 \end{pmatrix}$
	$\|\{bb\}^{\bar{3}}_{1}\{\bar{c}\,\bar{c}\}^{3}_{1}\rangle^{0}_{0}$	
1^{+}	$\|\{bb\}^{\bar{3}}_{1}\{\bar{c}\,\bar{c}\}^{3}_{1}\rangle^{0}_{1}$	(12960)
2^{+}	$\|\{bb\}^{\bar{3}}_{1}\{\bar{c}\,\bar{c}\}^{3}_{1}\rangle^{0}_{2}$	(12972)

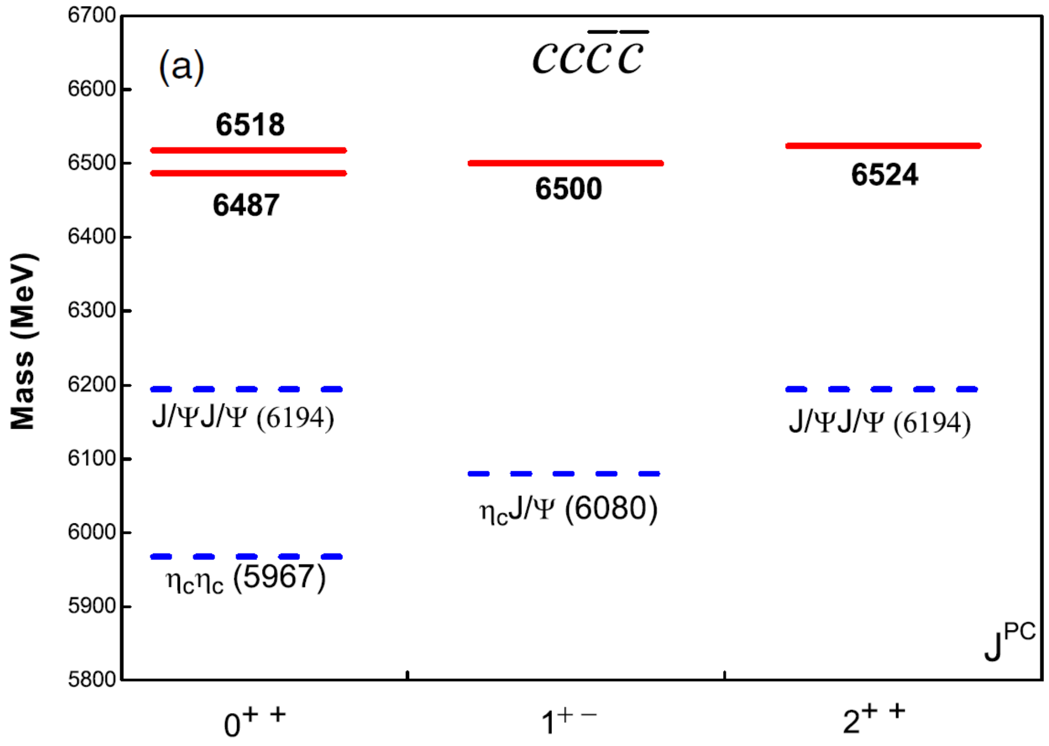

The transition between color representations $\mathbf{6} \otimes \bar{\mathbf{6}}$ and $\mathbf{3} \otimes \bar{\mathbf{3}}$ seems to be small.

G.J. Wang, L. Meng, M. Oka, S.L. Zhu, PRD 104, 036016 (2021)

For excited states of the 4-quark system, the spectra become complicated and crowded.

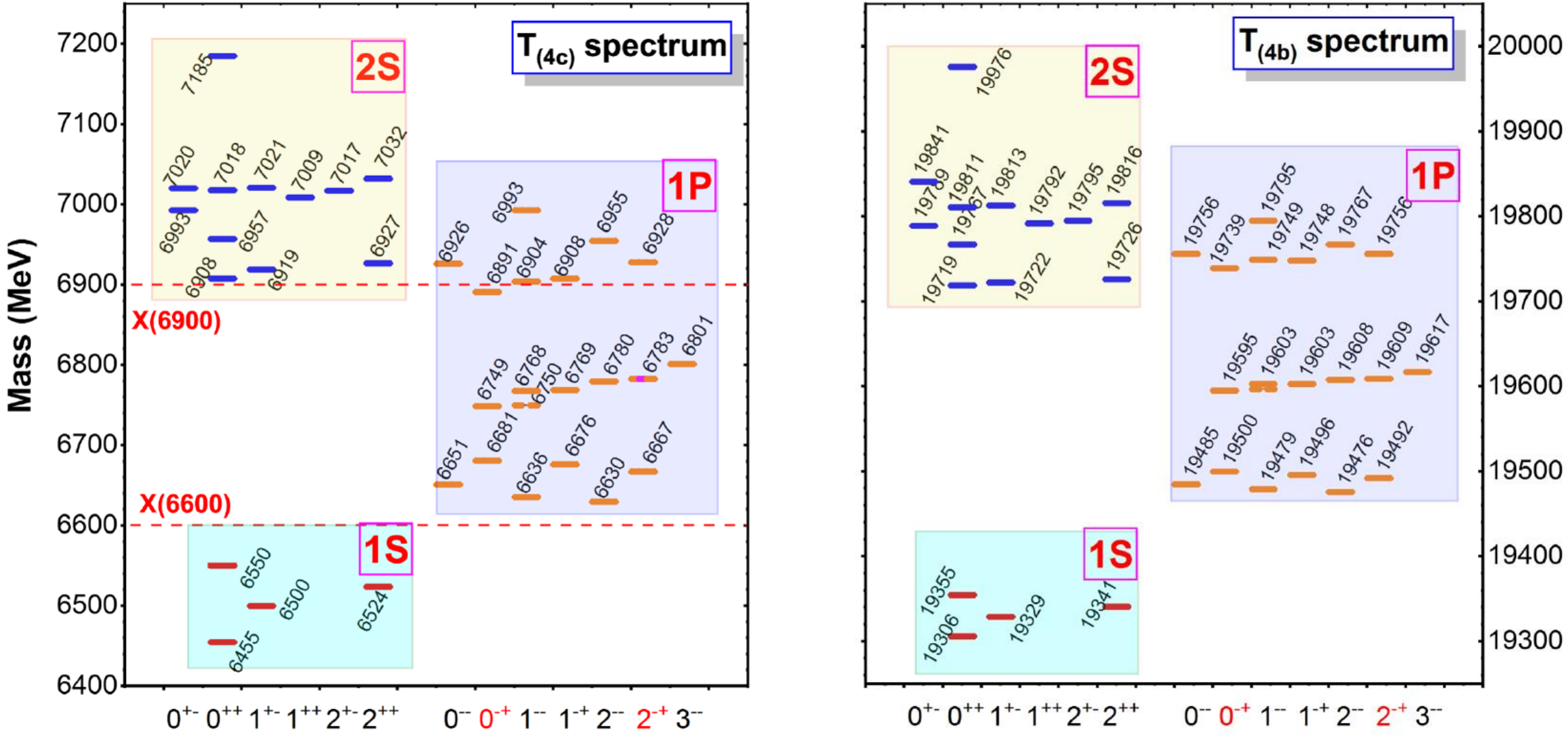

M.S. Liu, F.X. Liu, X.H. Zhong and Q. Zhao, 2006.11952 [hep-ph], PRD 109, 076017 (2024).
F.X. Liu, M.S. Liu, X.H. Zhong, and Q. Zhao, PRD 104, 116029 (2021)

First orbital excitation states

The radial part of the wavefunction is expanded with a series of harmonic oscillator functions:

$$R_{n_\xi l_\xi}(\xi) = \sum_{\ell=1}^{n} C_{\xi\ell}\, \phi_{n_\xi l_\xi}(d_{\xi\ell}, \xi),$$

where

$$\phi_{n_\xi l_\xi}(d_{\xi\ell}, \xi) = \left(\frac{1}{d_{\xi\ell}}\right)^{\frac{3}{2}} \left[\frac{2^{l_\xi+2-n_\xi}(2l_\xi+2n_\xi+1)!!}{\sqrt{\pi} n_\xi![(2l_\xi+1)!!]^2}\right]^{\frac{1}{2}} \left(\frac{\xi}{d_{\xi\ell}}\right)^{l_\xi} \times e^{-\frac{1}{2}\left(\frac{\xi}{d_{\xi\ell}}\right)^2} F\left(-n_\xi, l_\xi + \frac{3}{2}, \left(\frac{\xi}{d_{\xi\ell}}\right)^2\right),$$

Parameter $d_{\xi l}$ is oscillator length and is related to the harmonic oscillator frequency $\omega_{\xi l}$:

$$\frac{1}{d_{\xi l}^2} = M_\xi \omega_{\xi l}$$

The number of harmonic oscillator functions n is fitted together with $d_{\xi l}$ with $l = 1, 2, \ldots n$, via relation: $d_{\xi l} = d_{\xi 1} a^{l-1}$, with a the ratio coefficient.

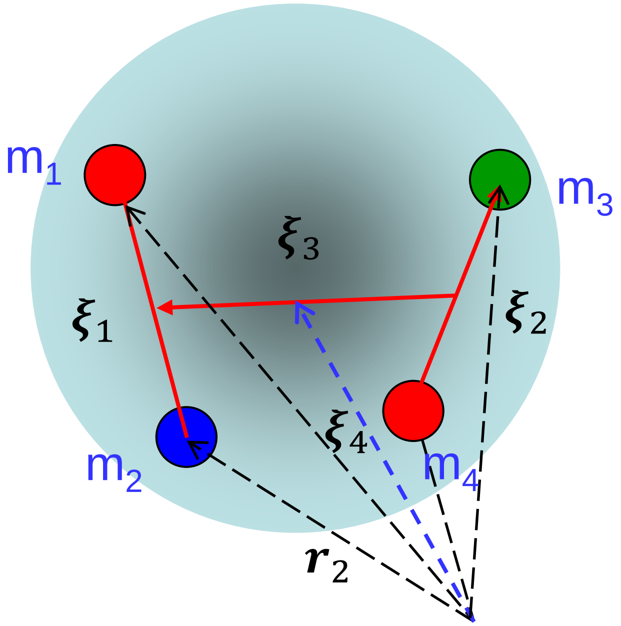

Jacobi coordinate

With $\boldsymbol{S} = 0, 1, 2$, and $\boldsymbol{L} = 1$, the total spin of a tetraquark state can be: $\boldsymbol{J} = \boldsymbol{S} + \boldsymbol{L} = 0, 1, 2, 3$.

Predicted masses for the *P*-wave $cc\bar{c}\bar{c}$ states. (ξ_1, ξ_2) stands for a configuration containing both ξ_1 and ξ_2-mode of orbital excitations, while (ξ_3) stands for a configuration containing ξ_3-mode of orbital excitation.

$J^{P(C)}$	Configuration	$\langle H \rangle$ (MeV)	Mass (MeV)	Eigenvector
0^{--}	$^3P_{0^{--}(6\bar{6})_c(\xi_1,\xi_2)}$ $^3P_{0^{--}(\bar{3}3)_c(\xi_1,\xi_2)}$	$\begin{pmatrix} 6751 & -132 \\ -132 & 6827 \end{pmatrix}$	$\begin{pmatrix} 6651 \\ 6926 \end{pmatrix}$	$\begin{pmatrix} (-0.7985 & -0.6020) \\ (-0.6020 & 0.7985) \end{pmatrix}$
0^{-+}	$^3P_{0^{-+}(6\bar{6})_c(\xi_1,\xi_2)}$ $^3P_{0^{-+}(\bar{3}3)_c(\xi_1,\xi_2)}$ $^3P_{0^{-+}(\bar{3}3)_c(\xi_3)}$	$\begin{pmatrix} 6746 & 88 & 37 \\ 88 & 6825 & 18 \\ 37 & 18 & 6750 \end{pmatrix}$	$\begin{pmatrix} 6681 \\ 6749 \\ 6891 \end{pmatrix}$	$\begin{pmatrix} (0.82 & -0.47 & -0.32) \\ (-0.14 & 0.38 & 0.91) \\ (0.55 & 0.80 & 0.25) \end{pmatrix}$
1^{--}	$^3P_{1^{--}(6\bar{6})_c(\xi_1,\xi_2)}$ $^3P_{1^{--}(\bar{3}3)_c(\xi_1,\xi_2)}$ $^5P_{1^{--}(\bar{3}3)_c(\xi_3)}$ $^1P_{1^{--}(\bar{3}3)_c(\xi_3)}$ $^1P_{1^{--}(6\bar{6})_c(\xi_3)}$	$\begin{pmatrix} 6733 & 132 & -29 & -16 & 31 \\ 132 & 6827 & -14 & -7 & 26 \\ -29 & -14 & 6754 & -3 & 10 \\ -16 & -7 & -3 & 6770 & -19 \\ 31 & 26 & 10 & -19 & 6968 \end{pmatrix}$	$\begin{pmatrix} 6636 \\ 6750 \\ 6768 \\ 6904 \\ 6993 \end{pmatrix}$	$\begin{pmatrix} (0.82 & -0.55 & 0.12 & 0.06 & -0.03) \\ (0.02 & -0.24 & -0.96 & -0.16 & 0.06) \\ (-0.01 & 0.05 & -0.17 & 0.98 & 0.10) \\ (-0.48 & -0.69 & 0.19 & 0.02 & 0.50) \\ (0.31 & 0.39 & -0.02 & -0.11 & 0.86) \end{pmatrix}$
1^{-+}	$^3P_{1^{-+}(6\bar{6})_c(\xi_1,\xi_2)}$ $^3P_{1^{-+}(\bar{3}3)_c(\xi_1,\xi_2)}$ $^3P_{1^{-+}(\bar{3}3)_c(\xi_3)}$	$\begin{pmatrix} 6751 & -108 & 9 \\ -108 & 6834 & -4 \\ 9 & -4 & 6769 \end{pmatrix}$	$\begin{pmatrix} 6676 \\ 6769 \\ 6908 \end{pmatrix}$	$\begin{pmatrix} (0.82 & 0.56 & -0.05) \\ (-0.01 & -0.08 & -1.00) \\ (-0.57 & 0.82 & -0.06) \end{pmatrix}$
2^{--}	$^3P_{2^{--}(6\bar{6})_c(\xi_1,\xi_2)}$ $^3P_{2^{--}(\bar{3}3)_c(\xi_1,\xi_2)}$ $^5P_{2^{--}(\bar{3}3)_c(\xi_3)}$	$\begin{pmatrix} 6746 & -155 & -18 \\ -155 & 6837 & 9 \\ -18 & 9 & 6781 \end{pmatrix}$	$\begin{pmatrix} 6630 \\ 6780 \\ 6955 \end{pmatrix}$	$\begin{pmatrix} (0.80 & 0.59 & 0.06) \\ (-0.01 & 0.12 & -1.00) \\ (-0.60 & 0.80 & 0.10) \end{pmatrix}$
2^{-+}	$^3P_{2^{-+}(6\bar{6})_c(\xi_1,\xi_2)}$ $^3P_{2^{-+}(\bar{3}3)_c(\xi_1,\xi_2)}$ $^3P_{2^{-+}(\bar{3}3)_c(\xi_3)}$	$\begin{pmatrix} 6754 & 123 & 12 \\ 123 & 6841 & 6 \\ 12 & 6 & 6783 \end{pmatrix}$	$\begin{pmatrix} 6667 \\ 6783 \\ 6928 \end{pmatrix}$	$\begin{pmatrix} (0.82 & -0.57 & -0.06) \\ (0.00 & 0.10 & -1.00) \\ (0.58 & 0.81 & 0.08) \end{pmatrix}$
3^{--}	$^5P_{3^{--}(\bar{3}3)_c(\xi_3)}$	(6801)	6801	1

X(6900) mass region

The contributions from each part of the Hamiltonian of the $cc\bar{c}\bar{c}$ systems in units of MeV with $L = 1$.

$J^{P(C)}$	Configuration	Mass	$\langle T \rangle$	$\langle V^{Conf} \rangle$	$\langle V^{OGE}_{coul} \rangle$	$\langle V^{OGE}_{SS} \rangle$	$\langle V^{OGE}_{tensor} \rangle$	$\langle V^{OGE}_{LS} \rangle$
0^{--}	$^3P_{0^{--}(6\bar{6})_c(\xi_1,\xi_2)}$	6751	717	778	−686	1.62	12.92	−4.31
	$^3P_{0^{--}(\bar{3}3)_c(\xi_1,\xi_2)}$	6827	741	810	−651	0.62	3.04	−9.11
0^{-+}	$^3P_{0^{-+}(6\bar{6})_c(\xi_1,\xi_2)}$	6746	727	773	−691	11.59	−1.48	−4.43
	$^3P_{0^{-+}(\bar{3}3)_c(\xi_1,\xi_2)}$	6825	745	808	−653	4.70	−3.07	−9.21
	$^3P_{0^{-+}(\bar{3}3)_c(\xi_3)}$	6750	765	769	−694	4.22	−6.45	−19.35
1^{--}	$^3P_{1^{--}(6\bar{6})_c(\xi_1,\xi_2)}$	6733	743	765	−699	1.73	−6.89	−2.30
	$^3P_{1^{--}(\bar{3}3)_c(\xi_1,\xi_2)}$	6827	741	810	−651	0.62	−1.52	−4.55
	$^5P_{1^{--}(\bar{3}3)_c(\xi_3)}$	6754	761	771	−692	15.62	−4.47	−28.76
	$^1P_{1^{--}(\bar{3}3)_c(\xi_3)}$	6770	734	784	−679	−1.38	0	0
	$^1P_{1^{--}(6\bar{6})_c(\xi_3)}$	6968	714	885	−578	13.51	0	0
1^{-+}	$^3P_{1^{-+}(6\bar{6})_c(\xi_1,\xi_2)}$	6751	720	776	−688	11.45	0.73	−2.18
	$^3P_{1^{-+}(\bar{3}3)_c(\xi_1,\xi_2)}$	6834	732	815	−647	4.63	1.49	−4.46
	$^3P_{1^{-+}(\bar{3}3)_c(\xi_3)}$	6769	736	783	−680	4.03	3.01	−9.03
2^{--}	$^3P_{2^{--}(6\bar{6})_c(\xi_1,\xi_2)}$	6746	724	774	−690	1.65	1.32	2.19
	$^3P_{2^{--}(\bar{3}3)_c(\xi_1,\xi_2)}$	6837	725	819	−644	0.64	0.29	4.38
	$^5P_{2^{--}(\bar{3}3)_c(\xi_3)}$	6781	720	791	−672	14.38	4.05	−8.69
2^{-+}	$^3P_{2^{-+}(6\bar{6})_c(\xi_1,\xi_2)}$	6754	715	779	−685	11.35	−0.14	2.15
	$^3P_{2^{-+}(\bar{3}3)_c(\xi_1,\xi_2)}$	6841	722	821	−642	4.57	−0.29	4.35
	$^3P_{2^{-+}(\bar{3}3)_c(\xi_3)}$	6783	715	794	−670	3.89	−0.57	8.59
3^{--}	$^5P_{3^{--}(\bar{3}3)_c(\xi_3)}$	6801	692	807	−658	13.55	−1.08	16.20

- One still sees significant contributions from the confinement potential which push the energy level further beyond the two-heavy meson thresholds.

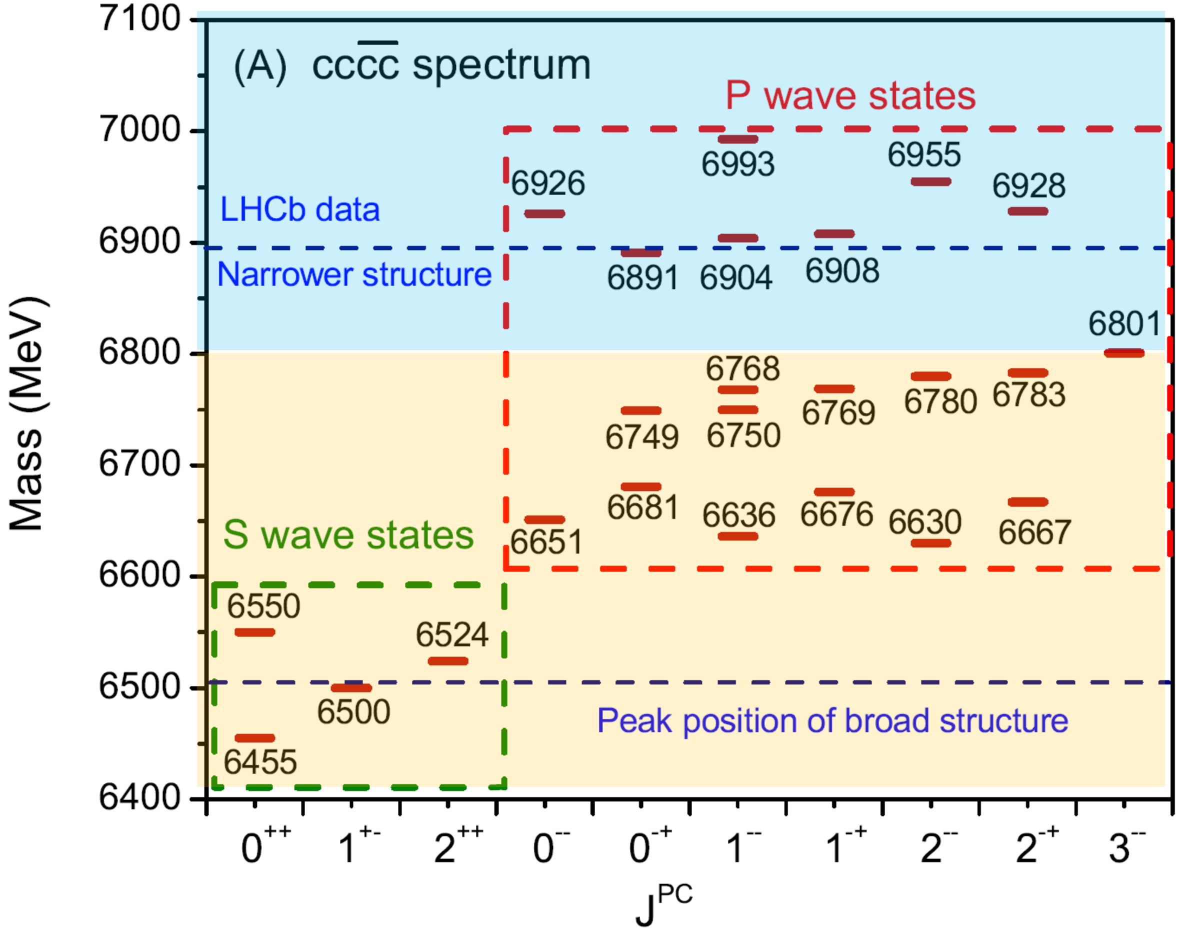
(A) $cc\bar{c}\bar{c}$ spectrum
P wave states
LHCb data
Narrower structure
S wave states
Peak position of broad structure
6550
6500
6524
6455
6926
6993
6955
6928
6891
6904
6908
6801
6768
6749
6750
6769
6780
6783
6651
6681
6636
6676
6630
6667
Mass (MeV)
7100
7000
6900
6800
6700
6600
6500
6400
0^{++} 1^{+-} 2^{++} 0^{--} 0^{-+} 1^{--} 1^{-+} 2^{--} 2^{-+} 3^{--}
J^{PC}

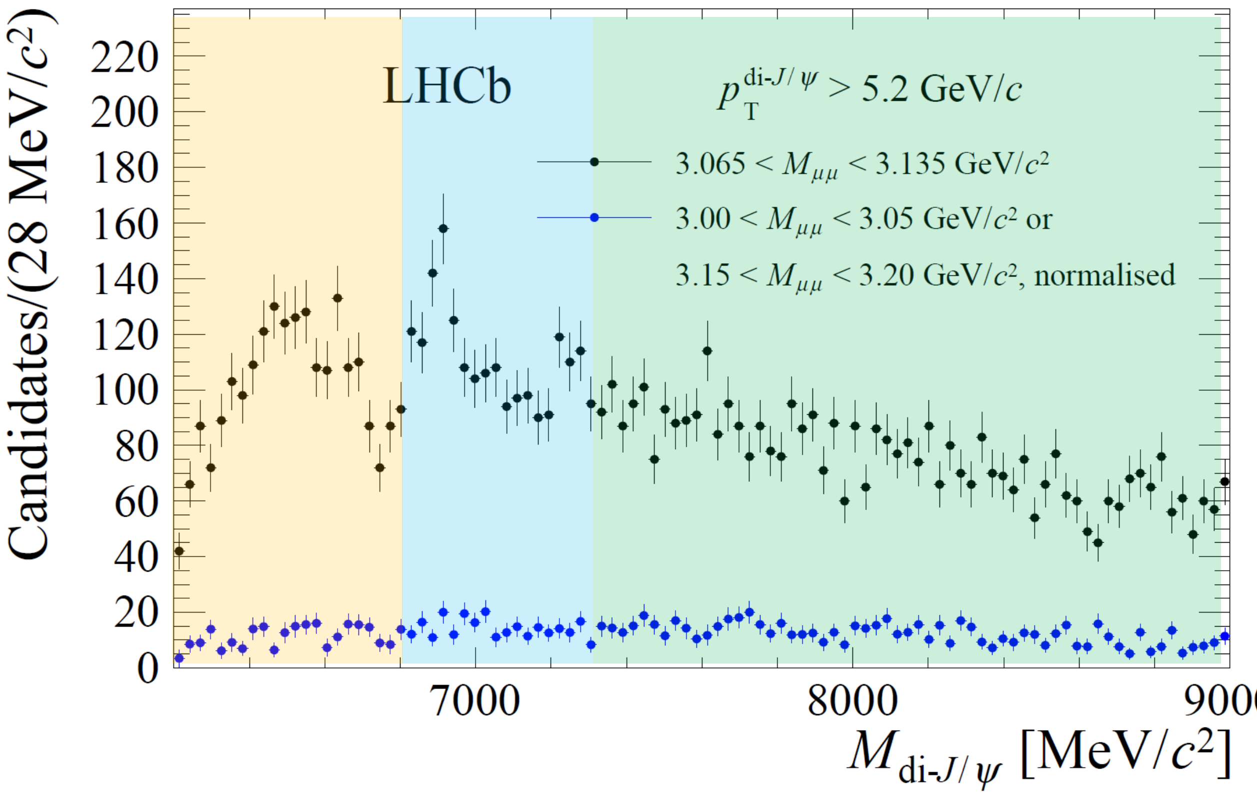
LHCb
$p_T^{\text{di-}J/\psi} > 5.2$ GeV/c
$3.065 < M_{\mu\mu} < 3.135$ GeV/c^2
$3.00 < M_{\mu\mu} < 3.05$ GeV/c^2 or
$3.15 < M_{\mu\mu} < 3.20$ GeV/c^2, normalised
Candidates/(28 MeV/c^2)
0
20
40
60
80
100
120
140
160
180
200
220
7000
8000
9000
$M_{\text{di-}J/\psi}$ [MeV/c^2]

Predicted mass spectrum for the 2S- and 3S-wave $T_{cc\bar{c}\bar{c}}$ states

J^{PC}	Configuration	$\langle H\rangle$ (MeV)	Mass (MeV)	Eigenvector
0^{+-}	$2^1S_{0^{+-}(6\bar{6})_c(\xi_1,\xi_2)}$ $2^1S_{0^{+-}(\bar{3}3)_c(\xi_1,\xi_2)}$	$\begin{pmatrix} 7008 & -14 \\ -14 & 7005 \end{pmatrix}$	$\begin{pmatrix} 6993 \\ 7020 \end{pmatrix}$	$\begin{pmatrix} -0.66 & -0.75 \\ -0.75 & 0.66 \end{pmatrix}$
0^{++}	$2^1S_{0^{++}(6\bar{6})_c(\xi_1,\xi_2)}$ $2^1S_{0^{++}(\bar{3}3)_c(\xi_1,\xi_2)}$ $2^1S_{0^{++}(6\bar{6})_c(\xi_3)}$ $2^1S_{0^{++}(\bar{3}3)_c(\xi_3)}$	$\begin{pmatrix} 6954 & -19 & 13 & -11 \\ -19 & 7000 & -4 & -36 \\ 13 & -4 & 7183 & -12 \\ -11 & -36 & -12 & 6930 \end{pmatrix}$	$\begin{pmatrix} 6908 \\ 6957 \\ 7018 \\ 7185 \end{pmatrix}$	$\begin{pmatrix} 0.35 & 0.40 & 0.03 & 0.84 \\ -0.91 & -0.05 & 0.07 & 0.41 \\ 0.21 & -0.91 & -0.01 & 0.35 \\ -0.06 & 0.02 & -1.00 & 0.05 \end{pmatrix}$
1^{+-}	$2^3S_{1^{+-}(\bar{3}3)_c(\xi_1,\xi_2)}$ $2^3S_{1^{+-}(\bar{3}3)_c(\xi_3)}$	$\begin{pmatrix} 7006 & -37 \\ -37 & 6934 \end{pmatrix}$	$\begin{pmatrix} 6919 \\ 7021 \end{pmatrix}$	$\begin{pmatrix} -0.39 & -0.92 \\ -0.92 & 0.39 \end{pmatrix}$
1^{++}	$2^3S_{1^{++}(\bar{3}3)_c(\xi_1,\xi_2)}$	(7009)	7009	1
2^{+-}	$2^5S_{2^{+-}(\bar{3}3)_c(\xi_1,\xi_2)}$	(7017)	7017	1
2^{++}	$2^5S_{2^{++}(\bar{3}3)_c(\xi_1,\xi_2)}$ $2^5S_{2^{++}(\bar{3}3)_c(\xi_3)}$	$\begin{pmatrix} 7018 & -36 \\ -36 & 6942 \end{pmatrix}$	$\begin{pmatrix} 6927 \\ 7032 \end{pmatrix}$	$\begin{pmatrix} -0.37 & -0.93 \\ -0.93 & 0.37 \end{pmatrix}$
0^{+-}	$3^1S_{0^{+-}(6\bar{6})_c(\xi_1,\xi_2)}$ $3^1S_{0^{+-}(\bar{3}3)_c(\xi_1,\xi_2)}$	$\begin{pmatrix} 7356 & 9 \\ 9 & 7396 \end{pmatrix}$	$\begin{pmatrix} 7354 \\ 7398 \end{pmatrix}$	$\begin{pmatrix} -0.98 & 0.21 \\ 0.21 & 0.98 \end{pmatrix}$
0^{++}	$3^1S_{0^{++}(6\bar{6})_c(\xi_1,\xi_2)}$ $3^1S_{0^{++}(\bar{3}3)_c(\xi_1,\xi_2)}$ $3^1S_{0^{++}(6\bar{6})_c(\xi_3)}$ $3^1S_{0^{++}(\bar{3}3)_c(\xi_3)}$	$\begin{pmatrix} 7347 & -10 & 1 & -4 \\ -10 & 7403 & 0 & 2 \\ 1 & 0 & 7720 & -6 \\ -4 & 2 & -6 & 7241 \end{pmatrix}$	$\begin{pmatrix} 7240 \\ 7346 \\ 7405 \\ 7720 \end{pmatrix}$	$\begin{pmatrix} 0.03 & -0.01 & 0.01 & 1.00 \\ -0.99 & -0.17 & 0 & 0.03 \\ 0.17 & -0.99 & 0 & -0.02 \\ 0 & 0 & -1.00 & 0.01 \end{pmatrix}$
1^{+-}	$3^3S_{1^{+-}(\bar{3}3)_c(\xi_1,\xi_2)}$ $3^3S_{1^{+-}(\bar{3}3)_c(\xi_3)}$	$\begin{pmatrix} 7406 & 3 \\ 3 & 7243 \end{pmatrix}$	$\begin{pmatrix} 7243 \\ 7406 \end{pmatrix}$	$\begin{pmatrix} 0.02 & -1.00 \\ -1.00 & -0.02 \end{pmatrix}$
1^{++}	$3^3S_{1^{++}(\bar{3}3)_c(\xi_1,\xi_2)}$	(7399)	7399	1
2^{+-}	$3^5S_{2^{+-}(\bar{3}3)_c(\xi_1,\xi_2)}$	(7405)	7405	1
2^{++}	$3^5S_{2^{++}(\bar{3}3)_c(\xi_1,\xi_2)}$ $3^5S_{2^{++}(\bar{3}3)_c(\xi_3)}$	$\begin{pmatrix} 7412 & 3 \\ 3 & 7248 \end{pmatrix}$	$\begin{pmatrix} 7248 \\ 7412 \end{pmatrix}$	$\begin{pmatrix} 0.02 & -1.00 \\ -1.00 & -0.02 \end{pmatrix}$

F.X. Liu, M.S. Liu, X.H. Zhong, and Q. Zhao, PRD 104, 116029 (2021)

Energy decomposition for the 0^{++} states in the ground state, and first and second radial excitations

	J^{PC}	Configuration	Mass	$\langle T\rangle$	$\langle V^{Lin}\rangle$	$\langle V^{Coul}\rangle$	$\langle V^{SS}\rangle$	$\langle V^{T}\rangle$	$\langle V^{LS}\rangle$
1S	0^{++}	$1^1S_{0^{++}(6\bar{6})_c}$	6518	715	664	-811	17.82		
		$1^1S_{0^{++}(\bar{3}3)_c}$	6487	756	646	-834	-12.79		
2S	0^{++}	$2^1S_{0^{++}(6\bar{6})_c(\xi_1,\xi_2)}$	6954	725	883	-598	11.39		
		$2^1S_{0^{++}(\bar{3}3)_c(\xi_1,\xi_2)}$	7000	774	919	-622	-3.790		
		$2^1S_{0^{++}(6\bar{6})_c(\xi_3)}$	7183	757	1010	-522	6.520		
		$2^1S_{0^{++}(\bar{3}3)_c(\xi_3)}$	6930	761	876	-642	2.560		
3S	0^{++}	$3^1S_{0^{++}(6\bar{6})_c(\xi_1,\xi_2)}$	7347	764	1097	-455	9.02		
		$3^1S_{0^{++}(\bar{3}3)_c(\xi_1,\xi_2)}$	7403	838	1150	-518	0.53		
		$3^1S_{0^{++}(6\bar{6})_c(\xi_3)}$	7720	855	1326	-397	4.59		
		$3^1S_{0^{++}(\bar{3}3)_c(\xi_3)}$	7241	815	1064	-575	4.46		

For 0^{++},

$$\left|\frac{\langle V^{Lin}\rangle}{\langle V^{Coul}\rangle}\right|_{1S} \simeq 0.77\sim0.81$$

$$\left|\frac{\langle V^{Lin}\rangle}{\langle V^{Coul}\rangle}\right|_{2S} \simeq 1.36\sim1.93$$

$$\left|\frac{\langle V^{Lin}\rangle}{\langle V^{Coul}\rangle}\right|_{3S} \simeq 1.85\sim3.34$$

Fast growth of the linear confinement potential with the excitation quantum numbers

F.X. Liu, M.S. Liu, X.H. Zhong, and Q. Zhao, PRD 104, 116029 (2021)

Stability of the fully-heavy tetraquark states:

- Rearrangement decays

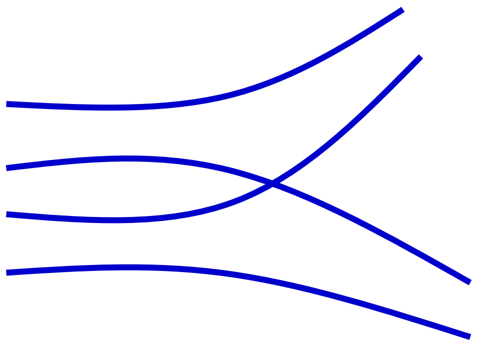

$M_T - 4m_Q > 2M_{c\bar{c}}$

- Two pion production

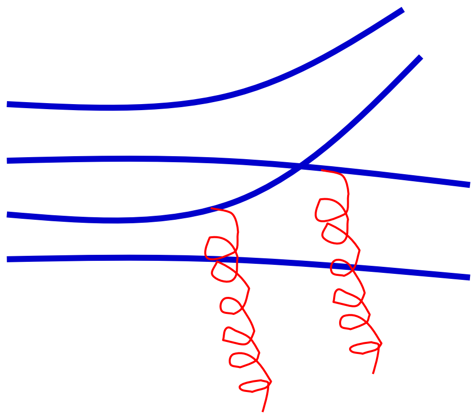

$M_T - 4m_Q > 2M_{c\bar{c}} + 2M_{\pi}$

Open channel decays

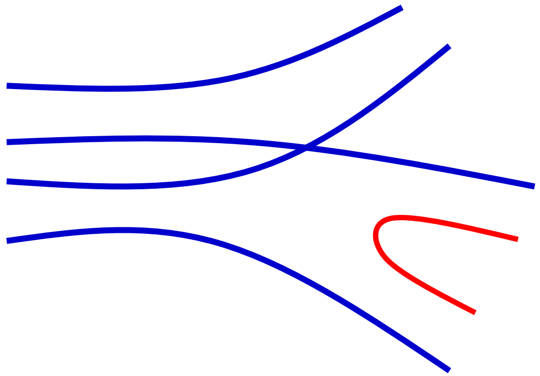

$M_T - 4m_Q > M_{c\bar{c}} + 2M_D$

Broad widths are expected for higher excitation multiquark states.

- States above the meson pair thresholds can decay via the fall-apart decay mechanism.
- For the fully-charmed tetraquark states, the calculation suggests that the ground states are above the charmonium pair thresholds.

$$\mathcal{M}(A \to BC) = -\sqrt{(2\pi)^3}\sqrt{8M_A E_B E_C}\langle BC|\sum_{i<j} V_{ij}|A\rangle$$

$$\langle BC|V_{ij}|A\rangle = \left(\left\langle \frac{1}{\sqrt{3}}[\chi^1_{11}\chi^2_{1-1} - \chi^1_{10}\chi^2_{10} + \chi^1_{1-1}\chi^2_{11}][11]_c \right| \hat{O}^{sc}_{ij} \left| c_1\chi^{00}_{00}[6\bar{6}] + c_2\chi^{11}_{00}[\bar{3}3]_c \right\rangle\right) \langle \varphi^1_{000}\varphi^2_{000}\phi|\hat{O}^o_{ij}|\psi^{1S}_{000}\rangle, \qquad \text{(A4)}$$

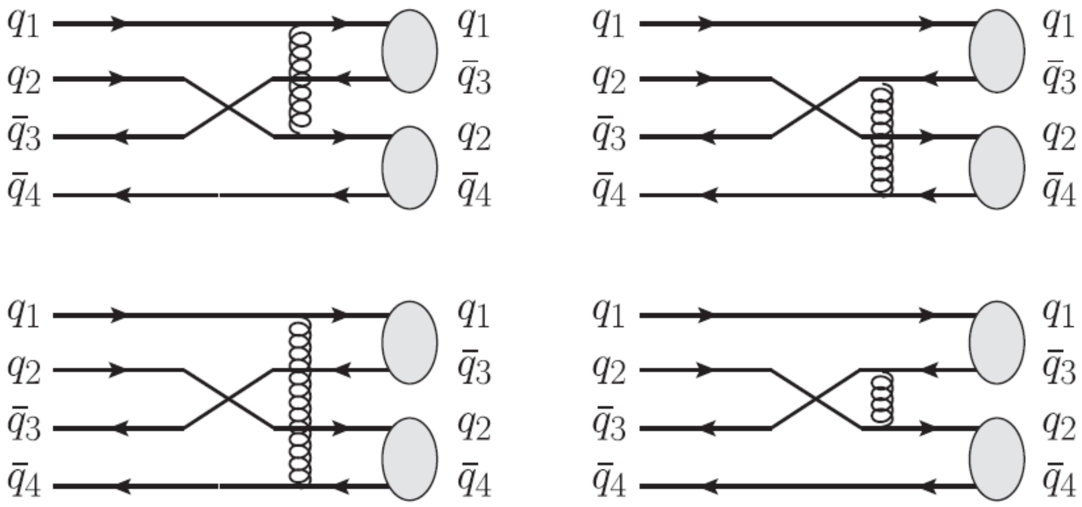

TABLE II. Fall-apart decay properties for the $T_{(4c)}$ states. The unit of the partial widths of each channel is MeV.

State	$\eta_c\eta_c$	$J/\psi J/\psi$	$\eta_c\eta_c(2S)$	$J/\psi\psi(2S)$	$\chi_{c0}\chi_{c0}/\chi_{c0}\chi_{c1}$	$\chi_{c0}\chi_{c2}/\chi_{c1}\chi_{c1}$	$\chi_{c1}\chi_{c2}/\chi_{c2}\chi_{c2}/h_c h_c$
$T_{(4c)0^{++}}(6455)(1S)$	1.45	0.70	⋯	⋯	⋯	⋯	⋯
$T_{(4c)0^{++}}(6550)(1S)$	0.12	1.78	⋯	⋯	⋯	⋯	⋯
$T_{(4c)2^{++}}(6524)(1S)$	⋯	0.00	⋯	⋯	⋯	⋯	⋯
$T_{(4c)0^{++}}(6908)(2S)$	0.61	0.12	0.55	0.09	22.5/⋯	⋯	⋯
$T_{(4c)0^{++}}(6957)(2S)$	0.01	4.66	0.05	3.17	70.8/⋯	⋯	⋯
$T_{(4c)0^{++}}(7018)(2S)$	3.14	1.87	0.00	0.07	14.8/⋯	0.00/⋯	⋯
$T_{(4c)0^{++}}(7185)(2S)$	0.00	0.48	0.21	0.14	1.14/⋯	0.05/6.12	0.53/18.0/5.79
$T_{(4c)2^{++}}(6927)(2S)$	⋯	0.36	⋯	0.30	0.00/1.15	⋯	⋯
$T_{(4c)2^{++}}(7032)(2S)$	⋯	7.12	⋯	2.83	0.23/98.0	325/214	⋯

State	$J/\psi J/\psi$	$\eta_c\chi_{c0}$	$\eta_c\chi_{c1}$	$\eta_c\chi_{c2}$	$J/\psi h_c$	$J/\psi\psi(2S)/\eta_c\eta_c(2S)$	$\chi_{c0}\chi_{c0}/\chi_{c0}\chi_{c1}/\chi_{c0}\chi_{c2}$
$T_{(4c)1^{++}}(7009)(2S)$	⋯	2.43	4.57	4.81	3.79	0.00/⋯	⋯/0.00/0.00
$T_{(4c)0^{-+}}(6681)(1P)$	0.04	1.28	0.00	0.03	0.40	⋯	⋯
$T_{(4c)0^{-+}}(6749)(1P)$	1.56	0.00	0.00	0.00	5.33	⋯	⋯
$T_{(4c)0^{-+}}(6891)(1P)$	0.00	2.38	0.00	0.79	0.06	0.00/⋯	0.00/⋯/⋯
$T_{(4c)1^{-+}}(6676)(1P)$	0.09	0.00	1.99	0.03	1.70	⋯/0.00	⋯
$T_{(4c)1^{-+}}(6769)(1P)$	0.21	0.00	1.22	0.06	5.57	⋯/0.00	⋯
$T_{(4c)1^{-+}}(6908)(1P)$	0.00	0.00	1.43	0.06	0.37	0.00/0.00	0.31/⋯/⋯
$T_{(4c)2^{-+}}(6667)(1P)$	0.00	0.02	0.03	0.05	0.03	⋯	⋯
$T_{(4c)2^{-+}}(6783)(1P)$	0.01	0.05	0.07	1.10	2.18	⋯	⋯
$T_{(4c)2^{-+}}(6928)(1P)$	0.01	0.05	0.08	0.88	1.98	0.00/⋯	0.00/⋯/⋯

state	$\eta_c J/\psi$	$\eta_c h_c$	$\chi_{c0} J/\psi$	$\chi_{c1} J/\psi$	$\chi_{c2} J/\psi$	$\eta_c \psi(2S)/\eta_c(2S) J/\psi$	$\chi_{c0} h_c$
$T_{(4c)1^{+-}}(6500)(1S)$	0.45	⋯	⋯	⋯	⋯	⋯/⋯	⋯
$T_{(4c)0^{+-}}(6993)(2S)$	⋯	3.16	3.45	2.65	0.54	⋯/⋯	⋯
$T_{(4c)0^{+-}}(7020)(2S)$	⋯	21.1	0.17	0.35	0.34	⋯/⋯	⋯
$T_{(4c)1^{+-}}(6919)(2S)$	0.05	⋯	0.02	0.04	0.06	0.09/0.68	⋯
$T_{(4c)1^{+-}}(7021)(2S)$	1.98	⋯	0.02	0.07	0.12	0.71/0.61	150
$T_{(4c)2^{+-}}(7017)(2S)$	⋯	⋯	4.70	3.75	0.86	⋯/⋯	⋯
$T_{(4c)0^{--}}(6651)(1P)$	0.24	⋯	0.00	6.75	⋯	⋯/⋯	⋯
$T_{(4c)0^{--}}(6926)(1P)$	0.12	⋯	0.02	2.76	0.19	0.00/0.00	⋯
$T_{(4c)1^{--}}(6636)(1P)$	0.04	0.02	3.28	0.97	⋯	⋯/⋯	⋯
$T_{(4c)1^{--}}(6750)(1P)$	0.17	0.01	1.92	3.99	1.05	0.00/0.00	⋯
$T_{(4c)1^{--}}(6768)(1P)$	0.00	2.77	0.08	0.99	0.79	0.00/0.00	⋯
$T_{(4c)1^{--}}(6904)(1P)$	0.00	0.17	2.96	0.26	0.17	0.00/0.00	⋯
$T_{(4c)1^{--}}(6993)(1P)$	0.03	1.91	0.12	0.76	1.49	0.00/0.00	0.17
$T_{(4c)2^{--}}(6630)(1P)$	0.06	0.01	0.01	0.02	⋯	⋯/⋯	⋯
$T_{(4c)2^{--}}(6780)(1P)$	0.01	0.01	0.01	3.55	2.00	0.00/0.00	⋯
$T_{(4c)2^{--}}(6955)(1P)$	0.00	0.00	0.11	1.75	3.45	0.00/0.01	0.00
$T_{(4c)3^{--}}(6801)(1P)$	0.00	0.00	0.16	0.27	11.8	0.00/0.00	⋯

The spatial size of the tetraquark states can be learned by calculating the root mean square radius $\sqrt{\langle r_{ij}^2 \rangle}$

TABLE VI. The components of different color configurations and the root mean square radii (fm) for each physical $T_{(4c)}$ states, where $\boldsymbol{r}_{12-34} \equiv (\mathbf{r}_1 + \mathbf{r}_2)/2 - (\mathbf{r}_3 + \mathbf{r}_4)/2$, $\boldsymbol{r}_{13-24} \equiv (\mathbf{r}_1 + \mathbf{r}_3)/2 - (\mathbf{r}_2 + \mathbf{r}_4)/2$.

State	$\vert 6\bar{6}\rangle_c$	$\vert \bar{3}3\rangle_c$	$\vert 11\rangle_c$	$\vert 88\rangle_c$	$\sqrt{\langle r_{12}^2\rangle}$	$\sqrt{\langle r_{12-34}^2\rangle}$	$\sqrt{\langle r_{13}^2\rangle}$	$\sqrt{\langle r_{13-24}^2\rangle}$
$T_{(4c)0^{++}}(6455)(1S)$	33.9%	66.1%	44.6%	55.4%	0.49	0.35	0.49	0.35
$T_{(4c)0^{++}}(6550)(1S)$	66.1%	33.9%	55.4%	44.6%	0.50	0.35	0.50	0.35
$T_{(4c)1^{+-}}(6500)(1S)$	0.0%	100.0%	33.3%	66.7%	0.50	0.35	0.50	0.35
$T_{(4c)2^{++}}(6524)(1S)$	0.0%	100.0%	33.3%	66.7%	0.51	0.36	0.51	0.36
$T_{(4c)0^{--}}(6651)(1P)$	64.0%	36.0%	54.7%	45.3%	0.63	0.39	0.59	0.45
$T_{(4c)0^{--}}(6926)(1P)$	36.0%	64.0%	45.3%	54.7%	0.63	0.39	0.59	0.45
$T_{(4c)0^{-+}}(6681)(1P)$	67.5%	32.5%	55.8%	44.2%	0.61	0.39	0.59	0.43
$T_{(4c)0^{-+}}(6749)(1P)$	2.0%	98.0%	34.0%	66.0%	0.55	0.47	0.61	0.39
$T_{(4c)0^{-+}}(6891)(1P)$	30.1%	69.9%	43.4%	56.6%	0.62	0.39	0.59	0.44
$T_{(4c)1^{--}}(6636)(1P)$	67.8%	32.2%	55.9%	44.1%	0.63	0.39	0.59	0.44
$T_{(4c)1^{--}}(6750)(1P)$	0.4%	99.6%	33.5%	66.5%	0.54	0.48	0.61	0.38
$T_{(4c)1^{--}}(6768)(1P)$	1.0%	99.0%	33.7%	663%.	0.55	0.50	0.63	0.39
$T_{(4c)1^{--}}(6904)(1P)$	48.4%	51.6%	49.5%	50.5%	0.60	0.42	0.60	0.43
$T_{(4c)1^{--}}(6993)(1P)$	83.5%	16.5%	61.2%	38.8%	0.57	0.47	0.62	0.4

(Table continued)

X(6450) mass region

Overall compact structures are observed.

TABLE VI. *(Continued)*

State	$\vert 6\bar{6}\rangle_c$	$\vert \bar{3}3\rangle_c$	$\vert 11\rangle_c$	$\vert 88\rangle_c$	$\sqrt{\langle r_{12}^2\rangle}$	$\sqrt{\langle r_{12-34}^2\rangle}$	$\sqrt{\langle r_{13}^2\rangle}$	$\sqrt{\langle r_{13-24}^2\rangle}$
$T_{(4c)1^{-+}}(6676)(1P)$	68.0%	32.0%	56.0%	44.0%	0.63	0.39	0.59	0.45
$T_{(4c)1^{-+}}(6769)(1P)$	0.0%	100.0%	33.3%	66.7%	0.55	0.50	0.63	0.39
$T_{(4c)1^{-+}}(6908)(1P)$	32.5%	67.5%	44.2%	55.8%	0.62	0.38	0.59	0.44
$T_{(4c)2^{--}}(6630)(1P)$	64.5%	35.5%	54.8%	45.2%	0.64	0.39	0.60	0.45
$T_{(4c)2^{--}}(6780)(1P)$	0.0%	100.0%	33.3%	66.7%	0.55	0.50	0.63	0.39
$T_{(4c)2^{--}}(6955)(1P)$	35.6%	64.4%	45.2%	54.8%	0.63	0.39	0.59	0.45
$T_{(4c)2^{-+}}(6667)(1P)$	67.2%	32.8%	55.7%	44.3%	0.63	0.39	0.59	0.45
$T_{(4c)2^{-+}}(6783)(1P)$	0.0%	100.0%	33.3%	66.7%	0.55	0.50	0.64	0.39
$T_{(4c)2^{-+}}(6928)(1P)$	33.7%	66.3%	44.6%	55.4%	0.63	0.39	0.59	0.45
$T_{(4c)3^{--}}(6801)(1P)$	0.0%	100.0%	33.3%	66.7%	0.56	0.51	0.64	0.39
$T_{(4c)0^{+-}}(6993)(2S)$	43.6%	56.4%	47.9%	52.1%	0.77	0.43	0.69	0.54
$T_{(4c)0^{+-}}(7020)(2S)$	56.4%	43.6%	52.1%	47.9%	0.78	0.42	0.69	0.55
$T_{(4c)0^{++}}(6908)(2S)$	12.5%	87.5%	37.5%	62.5%	0.45	0.66	0.73	0.32
$T_{(4c)0^{++}}(6957)(2S)$	83.0%	17.0%	61.0%	39.0%	0.76	0.42	0.69	0.54
$T_{(4c)0^{++}}(7018)(2S)$	4.4%	95.6%	34.8%	65.2%	0.56	0.56	0.69	0.40
$T_{(4c)0^{++}}(7185)(2S)$	99.7%	0.3%	66.6%	33.4%	0.74	0.33	0.62	0.52
$T_{(4c)1^{+-}}(6919)(2S)$	0.0%	100.0%	33.3%	66.7%	0.52	0.72	0.82	0.37
$T_{(4c)1^{+-}}(7021)(2S)$	0.0%	100.0%	33.3%	66.7%	0.69	0.36	0.61	0.49
$T_{(4c)1^{++}}(7009)(2S)$	0.0%	100.0%	33.3%	66.7%	0.73	0.45	0.68	0.51
$T_{(4c)2^{+-}}(7017)(2S)$	0.0%	100.0%	33.3%	66.7%	0.73	0.45	0.68	0.52
$T_{(4c)2^{++}}(6927)(2S)$	0.0%	100.0%	33.3%	66.7%	0.47	0.68	0.76	0.33
$T_{(4c)2^{++}}(7032)(2S)$	0.0%	100.0%	33.3%	66.7%	0.79	0.45	0.72	0.56

X(6900) mass region

3. Quark model states vs. hadronic molecules

Dynamics that can contribute in additional to the potential quark model Hamiltonian

Weinberg's compositeness theorem:

$$|\Psi\rangle = \begin{pmatrix} \lambda|\psi_0\rangle \\ \chi(\boldsymbol{k})|h_1 h_2\rangle \end{pmatrix}$$

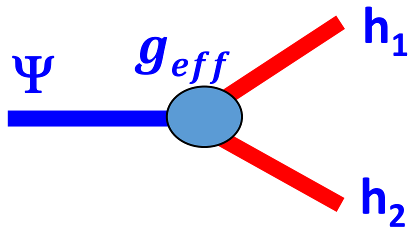

$$\hat{\mathcal{H}}|\Psi\rangle = E|\Psi\rangle, \qquad \hat{\mathcal{H}} = \begin{pmatrix} \hat{H}_c & \hat{V} \\ \hat{V} & \hat{H}^0_{hh} \end{pmatrix}$$

$\hat{H}^0_{hh} = k^2/(2\mu)$: two-hadron kinetic energy.

$\mu = m_1 m_2/(m_1 + m_2)$: two-hadron reduced mass.

$\langle\psi_0|\hat{V}|h_1 h_2\rangle = f(\boldsymbol{k})$: transition amplitude between the elementary component and two-hadron state.

Wave function in momentum space: $\chi(\boldsymbol{k}) = \lambda \dfrac{f(\boldsymbol{k})}{E - k^2/(2\mu)}$

Normalization of the physical wavefunction leads to the interpretation of the states mixings:

$$1 = \langle\Psi|\Psi\rangle = \lambda^2\langle\psi_0|\psi_0\rangle + \int \frac{d^3k}{(2\pi)^3}|\chi(\boldsymbol{k})|^2\langle h_1 h_2|h_1 h_2\rangle$$

$$= \lambda^2\left\{1 + \int \frac{d^3k}{(2\pi)^3}\frac{f^2(\boldsymbol{k})}{[E_B + k^2/(2\mu)]^2}\right\}.$$

$$E_B = m_1 + m_2 - M$$

$$\gamma = \sqrt{2\mu E_B}$$

Formation of hadronic molecules

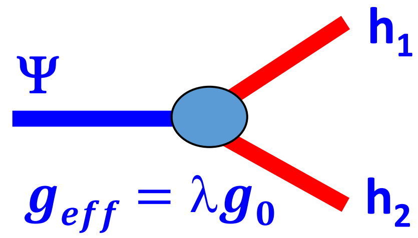

Given that the inverse range of force β >> γ (=$(2\mu E_B)^{1/2}$), the integral can be evaluated model independently for the case of S-wave coupling:

$$1 = \lambda^2 \left[1 + \frac{\mu^2 g_0^2}{2\pi\sqrt{2\mu E_B}} + \mathcal{O}\left(\frac{\gamma}{\beta}\right) \right] \qquad g_0 = f(0)$$

$$g_{eff}^2 \equiv \lambda^2 g_0^2 = \frac{2\pi\gamma}{\mu^2}(1-\lambda^2) = \frac{2\pi\gamma}{\mu^2}\chi^2$$

In the kinematic region of near threshold, a fixed E_B and sufficiently large g_0 imply a maximized rate for χ/λ. Note: Only with $E_B \to 0$, can it lead to $\lambda \to 0$. Otherwise, the physical state will always be associated with a compact component.

$$\Sigma(E) = -\int \frac{d^3k}{(2\pi)^3} \frac{f^2(\boldsymbol{k})}{E - k^2/(2\mu) + i\epsilon}$$

$$= \Sigma(-E_B) + i g_0^2 \frac{\mu}{2\pi} \sqrt{2\mu E + i\epsilon} + \mathcal{O}\left(\frac{\gamma}{\beta}\right)$$

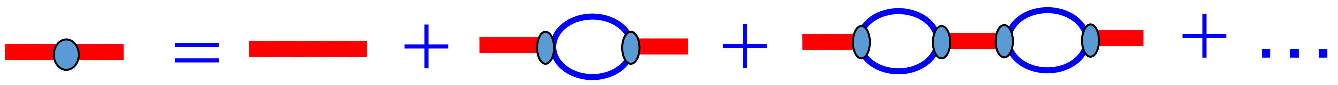

The molecular property, to some extent, needs a reasonably good understanding of the short-range component of the physical state.

T matrix for the two continuum hadron scattering:

$$T_{\rm NR}(E) = \frac{g_0^2}{E - E_0 + \Sigma(E)} + (\text{nonpole terms}) = \frac{g_0^2}{E + E_B + g_0^2\mu/(2\pi)(ik+\gamma)}$$

Quark-rearrangement couplings and final-state interactions

Bare couplings from QM

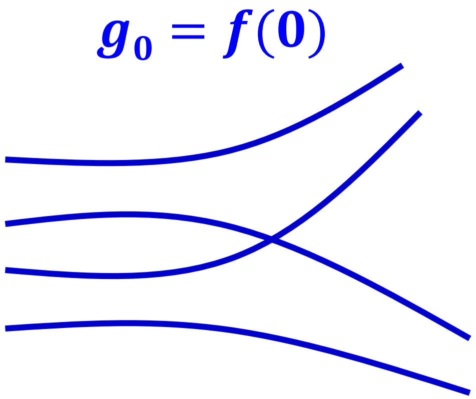

$$\langle \psi_0 | \hat{V} | h_1 h_2 \rangle = f(\boldsymbol{k})$$

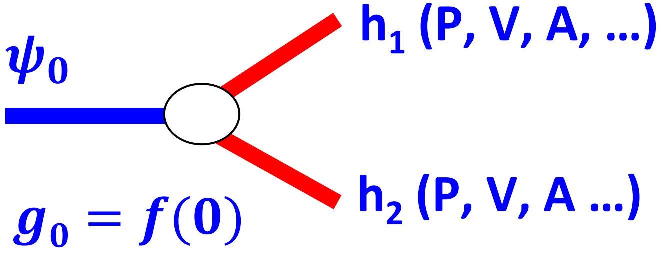

Physical couplings taking into account the FSIs

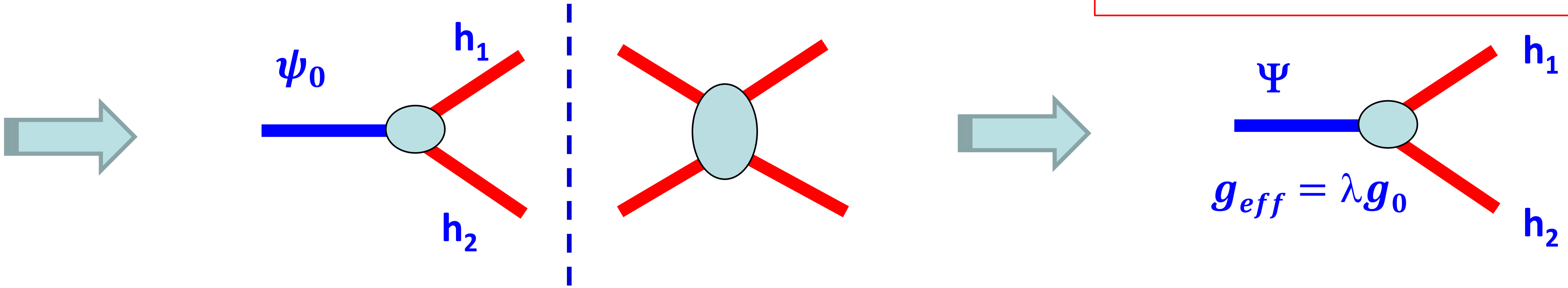

Unitarization of the FSI by solving the LS equation may generate structures near threshold, i.e. bound state, virtual state, or resonance. Tremendous efforts and a lot of publications on the hadronic molecules in recent years.

S wave thresholds and effects on the lineshapes

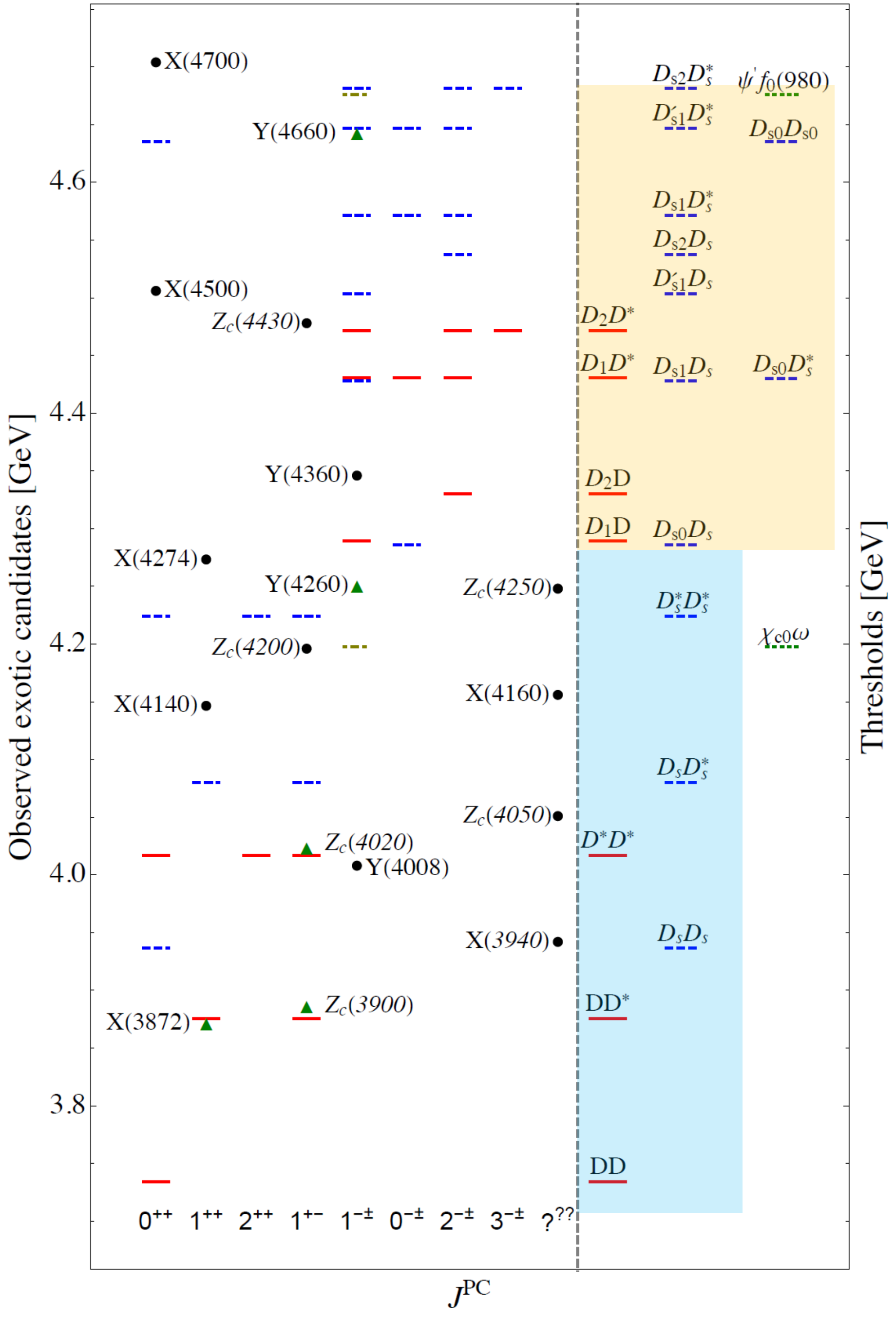

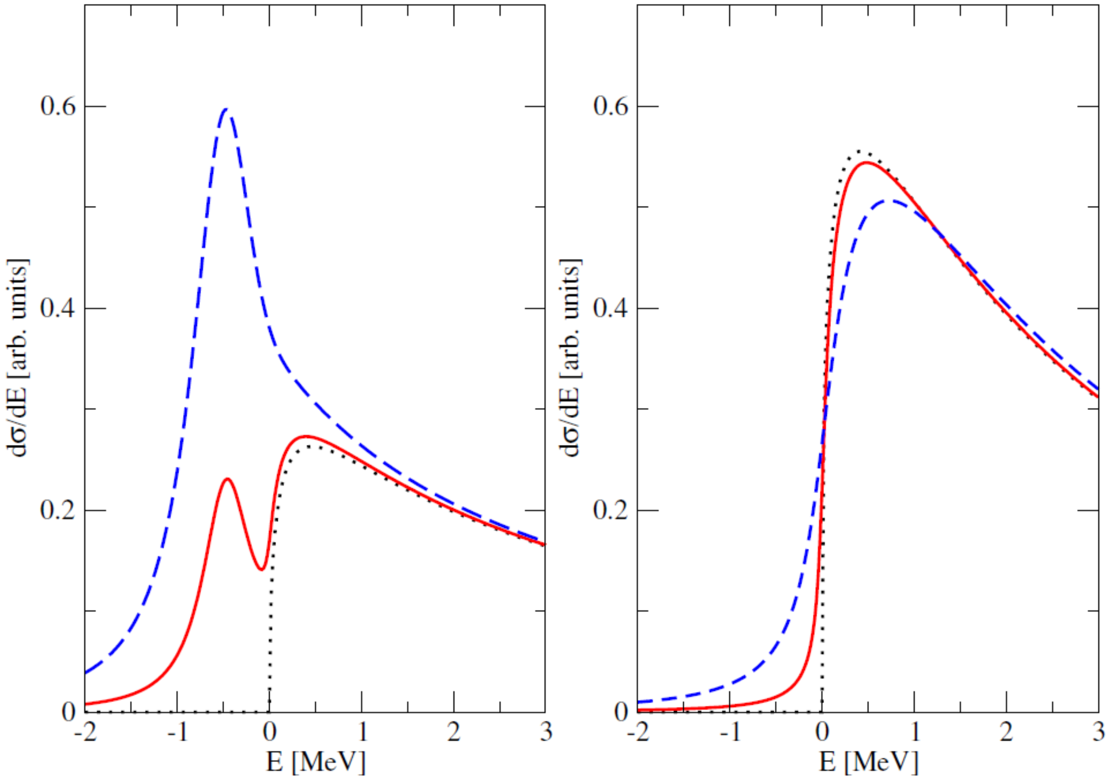

FIG. 10 Line shapes that emerge for a bound state (left panel) and for a virtual state (right panel) once one of the constituents is unstable. The dotted, solid and dashed line show the results for $\Gamma = 0, 0.1$ and 1 MeV, respectively. The other parameters of the calculation are given in Eq. (36).

F.-K. Guo, C. Hanhart, U.-G. Meissner, Q. Wang, Q. Zhao, B.-S. Zou, Rev. Mod. Phys. 90, 015004 (2018)

4. Some crucial issues to be noted

- Very rich spectra are expected.
- The form of diquark DoF can lead to very different results for the tetraquark production and decay.
- A strong coupling for a tetraquark state into a nearby S-wave threshold may need unitarization which will still introduce a molecular component into the wavefunction.
- Limited number of states close to threshold.
- Possible mixing with the kinematic singularity, but can be clarified by energy dependence of the lineshape measurement.
- Unitarization is crucial and EFT can be implemented. However, whether or not a molecular state can be formed would depend on the detailed dynamics.

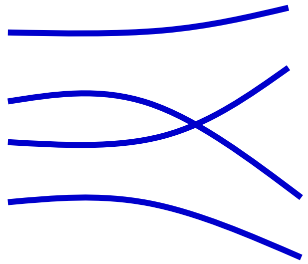

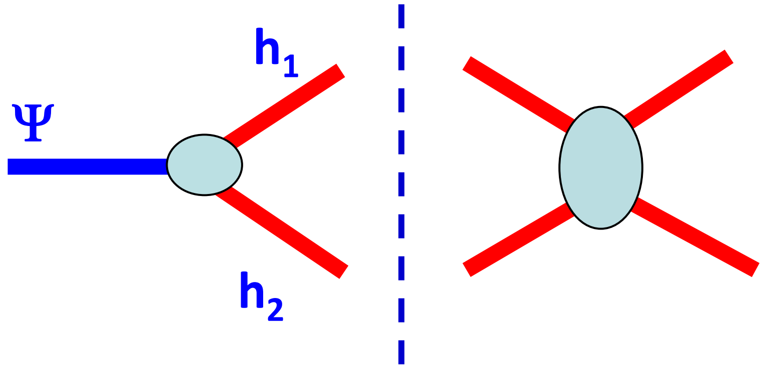

FB23 Website

http://fb23.ihep.ac.cn/

Overview

Circulars

Registration

Welcome Message

The 23rd International Conference on Few-Body Problems in Physics (FB23) will be held in Beijing, China on September 22-27, 2024, with Sept. 22 for registration. The registration website is https://indico.ihep.ac.cn/event/21083/registrations/1689/

Jointly organized by:

中国科学院高能物理研究所 Institute of High Energy Physics, Chinese Academy of Sciences

清華大學

中国科学院大学 University of Chinese Academy of Sciences

中国高等科学技术中心 China Center of Advanced Science and Technology

中国科学院理论物理研究所 Institute of Theoretical Physics, Chinese Academy of Sciences

華南師範大學 SOUTH CHINA NORMAL UNIVERSITY

中国物理学会 Chinese Physical Society

中国物理学会高能物理分会 HIGH ENERGY PHYSICS BRANCH OF CPS

Thanks for your attention!

Welcome to Beijing!

Recent reviews on hadron spectroscopy and QCD exotics:

1. F.K. Guo, C. Hanhart, U. G. Meißner, Q. Wang, Q. Zhao and B.S. Zou, Rev. Mod. Phys. 90, no.1, 015004 (2018);
2. H.X. Chen, W. Chen, X. Liu and S.L. Zhu, Phys. Rept. 639, 1-121 (2016);
3. A. Esposito, A. Pilloni and A. D. Polosa, Phys. Rept. 668, 1-97 (2017);
4. A. Ali, J.S. Lange and S. Stone, Prog. Part. Nucl. Phys. 97, 123-198 (2017);
5. Y.R. Liu, H. X. Chen, W. Chen, X. Liu and S.L. Zhu, Prog. Part. Nucl. Phys. 107, 237-320 (2019);
6. N. Brambilla, S. Eidelman, C. Hanhart, A. Nefediev, C.P. Shen, C.E. Thomas, A. Vairo and C.Z. Yuan, Phys. Rept. 873, 1-154 (2020);
7. R.F. Lebed, R.E. Mitchell and E.S. Swanson, Prog. Part. Nucl. Phys. 93, 143-194 (2017);
8. Y. Yamaguchi, A. Hosaka, S. Takeuchi and M. Takizawa, J. Phys. G 47, no.5, 053001 (2020).
9. R.M. Albuquerque, J.M. Dias, K.P. Khemchandani, A. Martinez Torres, F.S. Navarra, M. Nielsen and C. M. Zanetti, J. Phys. G 46, no.9, 093002 (2019)
10. F.-K. Guo, X.-H. Liu and S. Sakai, Prog. Part. Nucl. Phys. 112, 103757 (2020)

Thanks for your attention!

Coupled-channel explanations

Basic assumption:

Rescatterings of two charmonium states via a short-ranged potential would lead to near-threshold enhancements as either bound states, resonances, or virtual states.

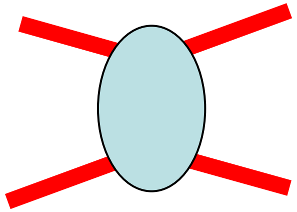

What is the dynamic origin of the short-ranged potential?

$$T(E) = V(E) \cdot [1 - G(E)V(E)]^{-1}$$

$$V_{2\mathrm{ch}}(E) = \begin{pmatrix} a_1 + b_1 k_1^2 & c \\ c & a_2 + b_2 k_2^2 \end{pmatrix}$$

$$V_{3\mathrm{ch}}(E) = \begin{pmatrix} a_{11} & a_{12} & a_{13} \\ a_{12} & a_{22} & a_{23} \\ a_{13} & a_{23} & a_{33} \end{pmatrix}$$

$$\mathcal{M}_1 = P(E)\left[1 + \sum_i r_i G_i(E) T_{i1}(E)\right] \qquad P(E) = \alpha e^{-\beta E^2}$$

$J/\psi\, J/\psi$, $J/\psi\, \psi(2S)$, $J/\psi\, \psi(1D)$

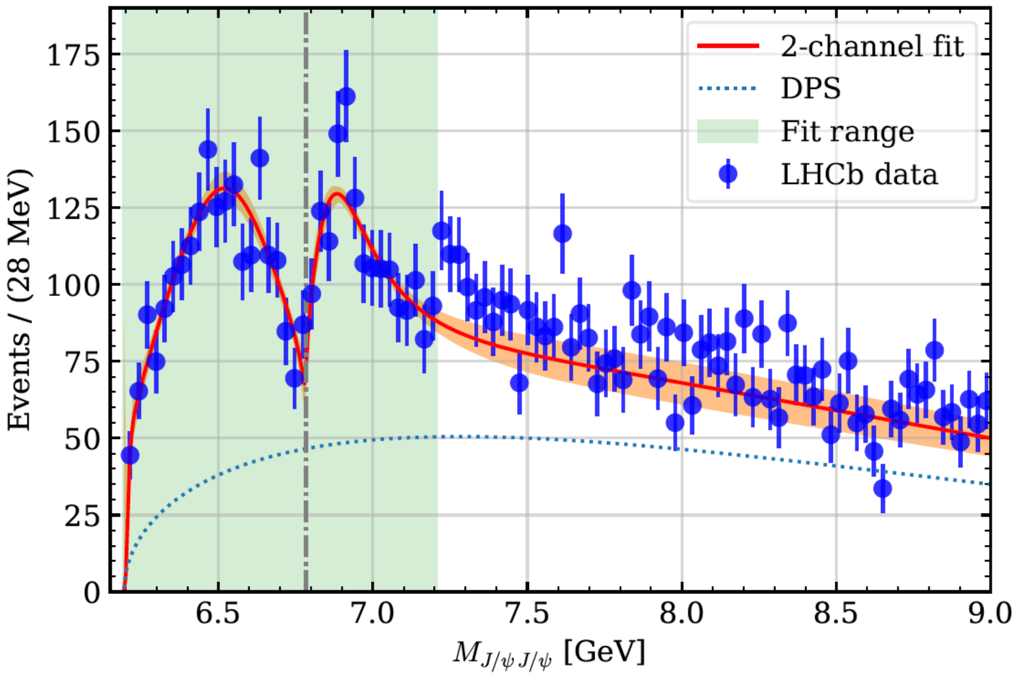

X.K. Dong, V. Baru, F. K. Guo, C. Hanhart and A. Nefediev, arXiv:2009.07795 [hep-ph]

1. Hadrons beyond the conventional quark model

Conventional QM states: Quantum numbers accessible by the quark-antiquark scenario:

States in **natural spin-parity**: if $P = (-1)^{L+1} = (-1)^J$.

Then with $S = 1$, one has $CP = (-1)^{(L+S)+(L+1)} = +1$

→ Mesons with **natural spin-parity** but $CP = -1$ will be forbidden:

$\mathbf{0^{+-}, 1^{-+}, 2^{+-}, 3^{-+}, \ldots}$

Exotic mesons:

Quantum numbers cannot be accessed by the spin-orbital couplings between a pair of $q\bar{q}$.

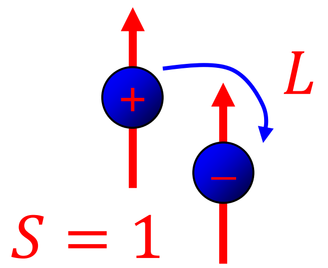

Natural: $0^{++}, 1^{--}, 2^{++}, 3^{--}, \ldots$

Unnatural: (0^{--}), $1^{++}, 2^{--}, 3^{++}, \ldots$

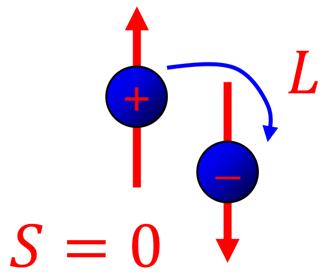

Unnatural: $0^{-+}, 1^{+-}, 2^{-+}, 3^{+-}, \ldots$

4. Some crucial issues to be noted

- **A genuine color-singlet multiquark state may not exist as a stable physical state. However, it should exist as the short-distance component in the physical state.**
- **With the increase of the constituents within the genuine color-singlet multiquark states they will become unstable due to the confinement potential.**
- **The nearby threshold may bring down the energy to stabilize the system which bridges it to the hadronic molecule scenario.**
- **The role played by the triangle singularity mechanism should be included in the analysis.**
- **LQCD can tell more…**
- **… …**

The connection between the quark model and QCD **ONLY** becomes clear in certain circumstances: in the heavy quark limit the soft QCD for quark-antiquark or quark-quark interactions can become much simpler.

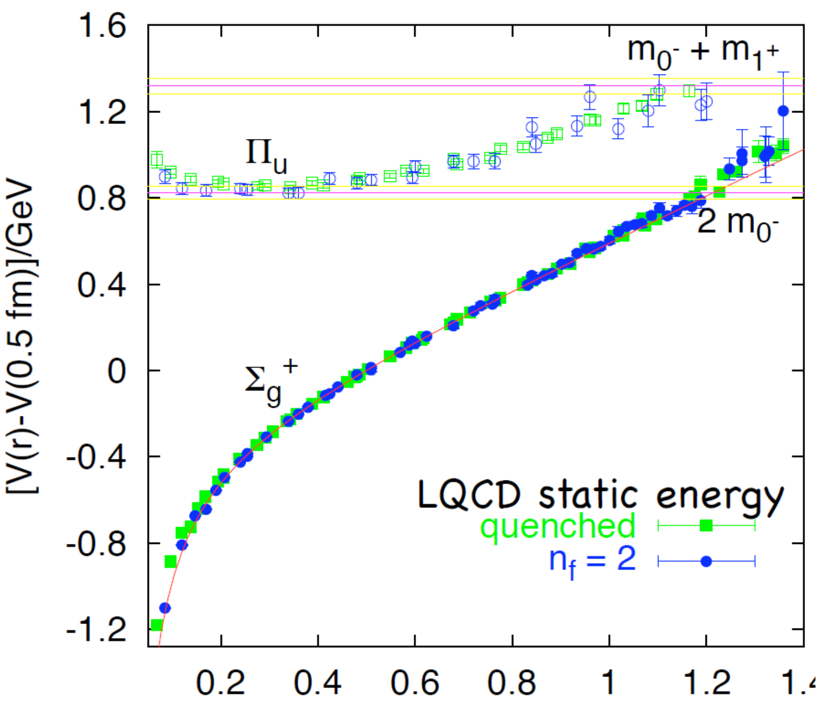

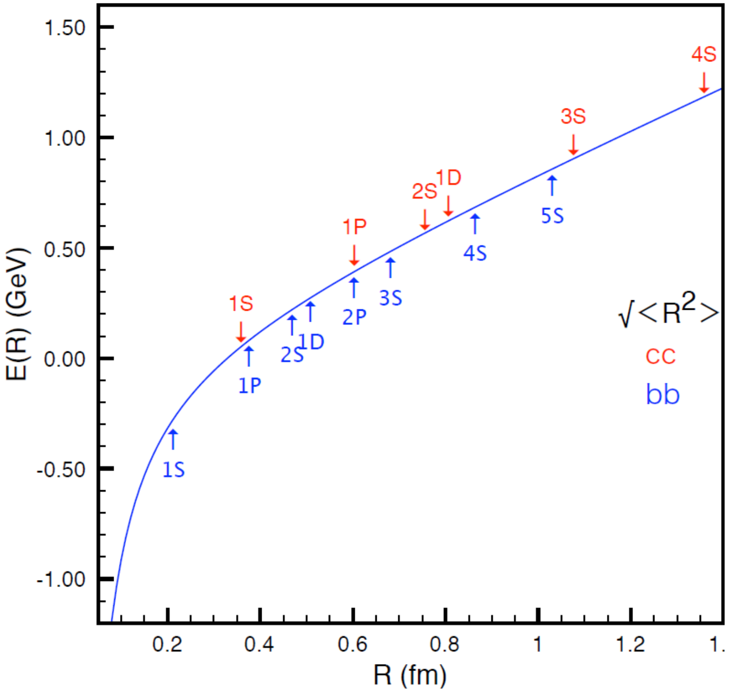

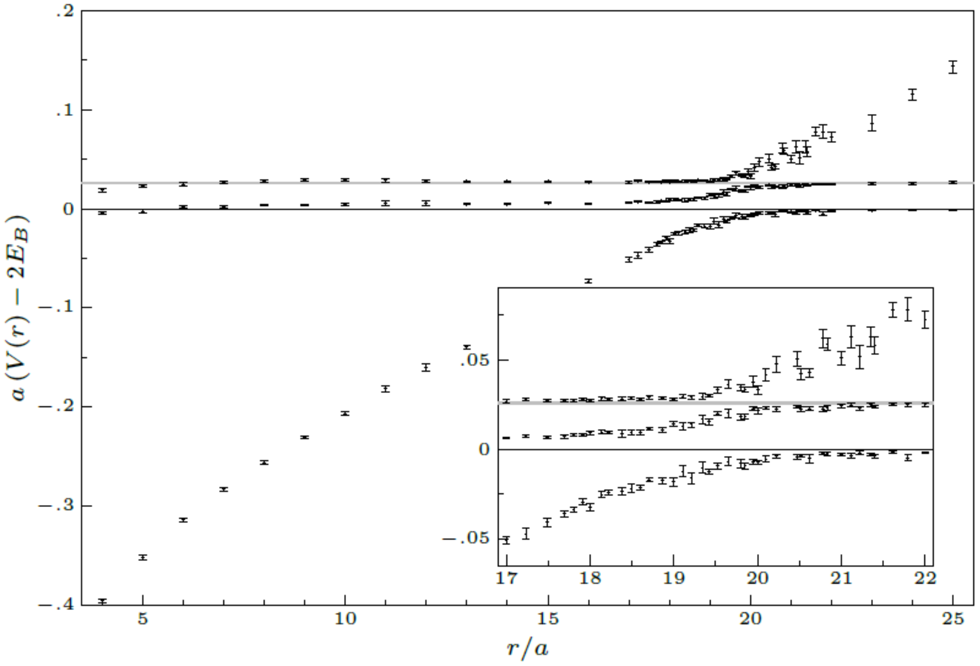

However, the effects of the open channels on the soft QCD potential is also evident!

G. S. Bali, et al., Phys. Rev. D62, 054503 (2000)
J. Bulava, et al., Phys. Lett. B793, 493 (2019),
M. Foster and C. Michael (UKQCD), Phys. Rev. D59, 094509 (1999)

Threshold phenomena and dynamics

- Color screening effects? String breaking effects? Unquenched effects? Coupled-channel effects?

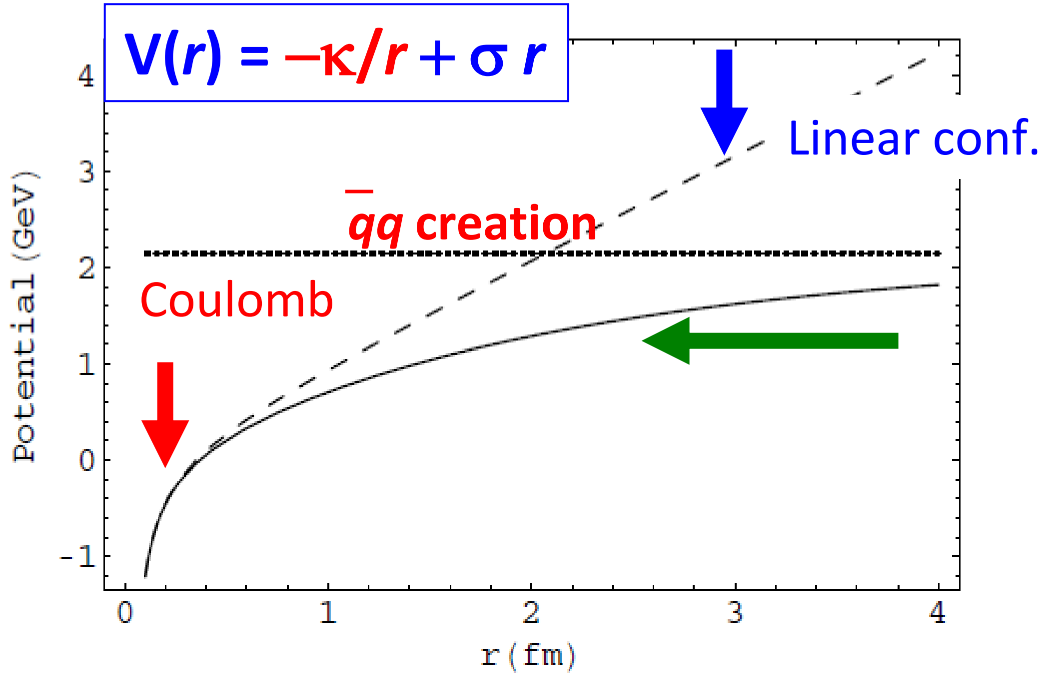

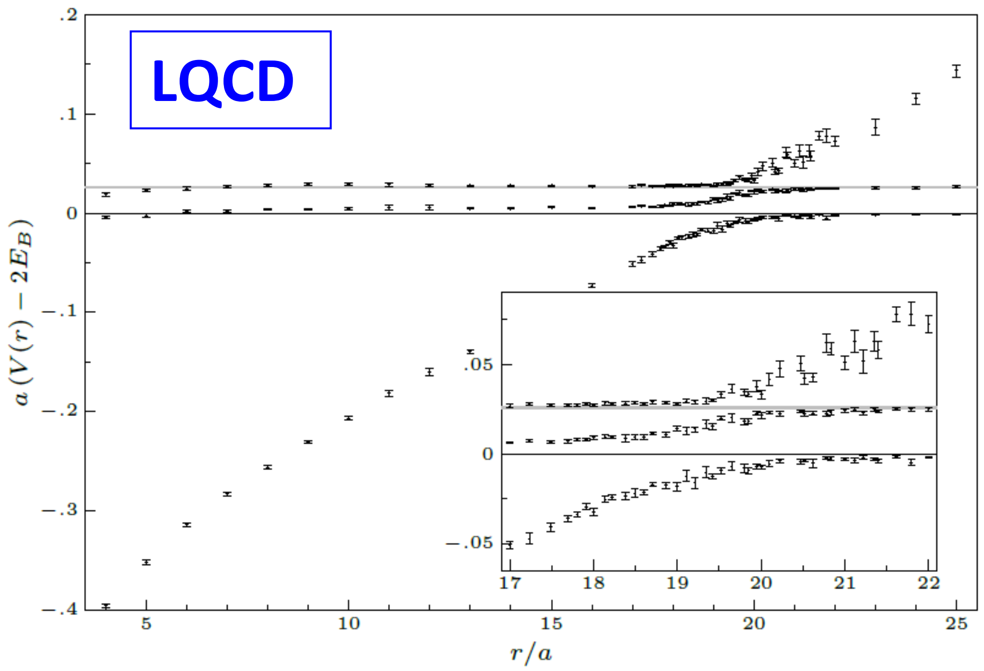

- **The effect of vacuum polarization due to dynamical quark pair creation may be manifested by the strong coupling to open thresholds and compensated by that of the hadron loops, i.e. coupled-channel effects.**

E. Eichten et al., PRD17, 3090 (1987)
E. J. Eichten, K. Lane, and C. Quigg, Phys. Rev. D 69, 094019 (2004)
B.-Q. Li and K.-T. Chao, Phys. Rev. D79, 094004 (2009);
T. Barnes and E. Swanson, Phys.Rev. C77, 055206 (2008)

Typical processes where the open threshold coupled channels can play a role

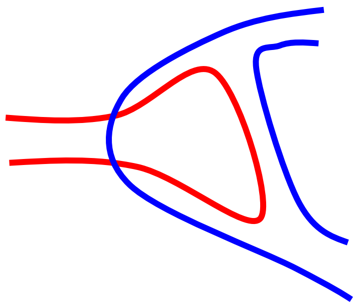

$\psi(3770) \to non D\bar{D}$

"ρπ puzzle"

Y.J. Zhang, G. Li, Q. Zhao, PRL(2009);
X. Liu, B. Zhang, X.Q. Li, PLB(2009)
Q. Wang et al. PRD(2012), PLB(2012)

$\chi_{c1} \to VV, \ \chi_{c2} \to VP$

X.-H. Liu et al, PRD81, 014017(2010);
X. Liu et al, PRD81, 074006(2010)

$\eta_c(\eta_c') \to VV$

Q. Wang et al, PRD2012

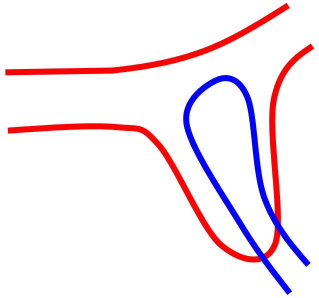

$\psi' \to J/\psi\pi^0, \psi' \to J/\psi\eta$

$\psi' \to \gamma\eta_c, J/\psi \to \gamma\eta_c$

G. Li and Q. Zhao, PRD(2011)074005
F.K. Guo, C. Hanhart, G. Li, U.-G. Meiβner and Q. Zhao, PRD82, 034025 (2010); PRD83, 034013 (2011)
F.K. Guo and Ulf-G Meiβner, PRL108(2012)112002

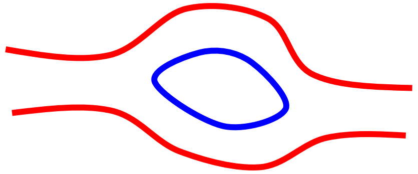

$D_{s1}(2460) - D_{s1}(2536)$

The mass shift in charmonia and charmed mesons, E.Eichten et al., PRD17(1987)3090
X.-G. Wu and Q. Zhao, PRD85, 034040 (2012)

The open channel couplings introduce NOT ONLY additional dynamics (add. effective DOF) into the hadron structures, BUT ALSO novel kinematic effects, i.e. triangle singularity …

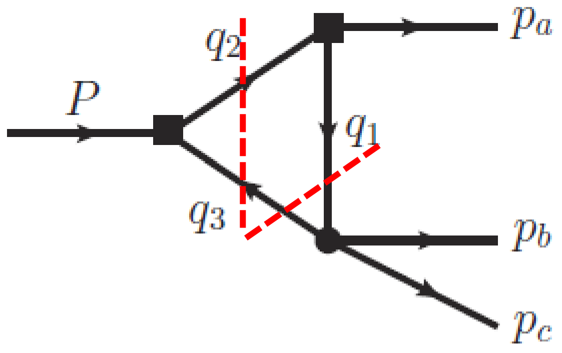

Exotics of Type-III:
Peak structures caused by kinematic effects, in particular, by triangle singularity.

$$\Gamma_3(s_1, s_2, s_3) = \frac{1}{i(2\pi)^4}\int \frac{d^4 q_1}{(q_1^2 - m_1^2 + i\epsilon)(q_2^2 - m_2^2 + i\epsilon)(q_3^2 - m_3^2 + i\epsilon)}$$
$$= \frac{-1}{16\pi^2}\int_0^1\int_0^1\int_0^1 da_1\, da_2\, da_3 \frac{\delta(1 - a_1 - a_2 - a_3)}{D - i\epsilon},$$

$$D \equiv \sum_{i,j=1}^{3} a_i a_j Y_{ij}, \quad Y_{ij} = \frac{1}{2}\left[m_i^2 + m_j^2 - (q_i - q_j)^2\right]$$

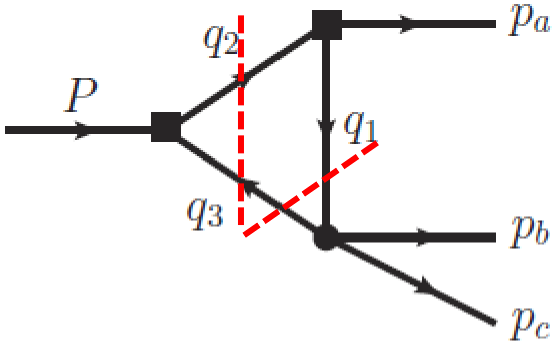

The TS occurs when all the three internal particles can approach their on-shell condition simultaneously:

$\partial D/\partial a_j = 0$ for all j=1,2,3. $\Rightarrow$ $\det[Y_{ij}] = 0$

L. D. Landau, Nucl. Phys. 13, 181 (1959);
J.J. Wu, X.-H. Liu, Q. Zhao, B.-S. Zou, Phys. Rev. Lett. 108, 081003 (2012);
Q. Wang, C. Hanhart, Q. Zhao, Phys. Rev. Lett. 111, 132003 (2013); Phys. Lett. B 725, 106 (2013)
X.-H. Liu, M. Oka and Q. Zhao, PLB753, 297(2016);
F.-K. Guo, C. Hanhart, U.-G. Meissner, Q. Wang, Q. Zhao, B.-S. Zou, arXiv:1705.00141[hep-ph], Rev. Mod. Phys. 90, 015004 (2018) ; F.-K. Guo, X.-H. Liu and S. Sakai, Prog. Part. Nucl. Phys. 112, 103757 (2020)